universität wien

DIPLOMARBEIT

Titel der Diplomarbeit

Characterisation of neuropathologic alterations following active immunotherapy against Aβ

angestrebter akademischer Grad

Magistra der Naturwissenschaften (Mag. rer.nat.)

Verfasserin / Verfasser:	Anna Gottenöf
Studienrichtung /Studienzweig (lt. Studienblatt):	A441 (Genetik/Mikrobiologie)
Betreuerin / Betreuer:	Univ.-Prof. Dr. Thomas Decker (Universität Wien)
	Dr. Markus Mandler (AFFiRiS AG)

Wien, im Dezember 2010

Abstract

Alzheimer's disease (AD) is the most common neurodegenerative disorder and the main cause of dementia. Diagnostic hallmarks of AD are neuritic plaques and neurofibrillary tangles in various regions of the brain. About 5% of the patients show mutations in genes involved in the pathogenesis of AD. These mutated genes were used to generate animal models for studying unclear mechanisms of the pathogenesis and to develop new treatment strategies for AD. In one of these models, the mouse model Tg2576, overexpression of human amyloid precursor protein (APP) carrying two point mutations leads to the development of amyloid plaques, the major hallmark of AD. One strategy to clear these plaques is active immunization. The vaccination of APP transgenic mice results in development of antibody titres highly specific against amyloid beta (Aβ), the main component of the amyloid plaques in the brain. This vaccination leads to lowering of AD pathology in mice.

AFFiRiS develops such vaccines based on the AFFITOPE technology which uses short peptides mimicking parts of the amyloid beta peptide that is produced naturally in the body. The induced antibodies bind with high affinity to Aβ and thereby clear the characteristic deposits. In addition the cognitive function of vaccinated animals is ameliorated compared to the transgenic untreated mice, which has been shown in behavioural test.

In this diploma thesis the impact of active AFFITOPE vaccination on different aspects of neuropathologic alterations in transgenic animals will be investigated. Among the examined parameters are different neurotransmitters, the structure and integrity of neurons, pre- and postsynaptic markers and the levels of neuroprotective factors. Changes concerning the structure and functionality of neurons could be determined by using the dendritic marker MAP2 in the immunofluorescence approach. Moreover, immunofluorescent staining of α-synuclein, a presynaptic protein, revealed alterations in its localisation and its grade of accumulation. Other postsynaptic factors, like PSD95, Drebrin and ARC/Arg3.1 were compared by Western Blotting showing no differences between wildtype and transgenic animals. Finally, neither in neurotransmitter nor in concentrations of the neuroprotective factor secreted APPα significant changes could be determined. In some synaptic markers pathologic alterations could be detected. The MAP2 density is lowered in transgenic animals compared to wildtype mice. In comparison with vaccinated animals trends towards the wildtype phenotype could be constituted. However, no significant differences were reached. The same is true for α-synuclein as a marker for

presynaptic alterations. Vaccinated transgenic animals show a decrease of these pathologic hallmarks. Concluding one can say that ameliorations of neuropathologic alterations could be detected in vaccinated animals.

Zusammenfassung

Die Alzheimer Krankheit (AD, engl. Alzheimer's Disease) ist die häufigste neurodegenerative Erkrankung und Verursacher von Demenz. Diagnostische Kennzeichen von AD sind neuritische Plaques und neurofibrilläre “tangles” in verschiedenen Hirnregionen. Circa 5% der AD-Patienten tragen Mutationen in Genen, die an der Pathogenese von AD beteiligt sind. Diese Mutationen werden genutzt um Tiermodelle zu generieren um unbekannte Mechanismen der Pathogenese zu studieren und um neue Behandlungsstrategien für AD zu entwickeln. In einem dieser Modelle, dem Mausmodell Tg2576, führt die Überexpression von humanem amyloiden Vorläuferprotein (APP), das zwei Punktmutationen trägt, zu der Entstehung von amyloiden Plaques, dem Hauptmerkmal von AD. Eine Möglichkeit die Plaques zu entfernen stellt die aktive Immuntherapie dar. Die Impfung APP transgener Mäuse führt zur Induktion von Antikörpertitern spezifisch gegen amyloid beta (Aβ), dem Hauptbestandteil der Plaques. Diese Impfung führt zu einer Reduktion der AD Pathologie.

AFFiRiS entwickelt solche Impfstoffe basierend auf der AFFITOPE Technologie, in der kurze Peptide benutzt werden, welche körpereigenes Aβ nachahmen. Die induzierten Antikörper binden mit hoher Affinität an Aβ und tragen dadurch zur Beseitigung der Ablagerungen bei. Zusätzlich konnte in Verhaltenstests eine Verbesserung der kognitiven Fähigkeiten der geimpften im Vergleich zu unbehandelten transgenen Mäusen gezeigt werden.

In dieser Diplomarbeit wurde der Einfluss der aktiven AFFITOPE Impfung auf verschiedene Aspekte neuropathologischer Veränderungen untersucht. Unter den betrachteten Faktoren befinden sich verschiedene Neurotransmitter, neuronale Struktur- und Integritätsindikatoren, prä- und postsynaptische Marker als auch neuroprotektive Faktoren. Bezüglich der Strukturen und Funktionalität von Neuronen konnten mit Hilfe des Dendritenmarkers MAP2 mit Hilfe von Immunfluoreszenzfärbungen Veränderungen nachgewiesen werden. Zudem konnten Veränderungen in der Lokalisation und der Anhäufung von α-synuclein, einem präsynaptischen Protein, mittels Immunfluoreszenz dargestellt werden. Andere postsynaptische Faktoren wie PSD95, Drebrin und ARC/Arg3.1 wurden mittels Western Blot in transgenen versus wildtyp Tieren verglichen. Letztendlich wurden weder in Neurotransmitterkonzentrationen noch in Levels des neuroprotektiven Faktors sAPPα signifikante Unterschiede in den verschieden behandelten Tieren gemessen. In einigen Synapsenmarkern konnten pathologische Veränderungen ge-

zeigt werden. Die MAP2 Dichte ist in transgenen Tieren im Vergleich zu Wildtype verringert. In geimpften transgenen Tieren konnte ein Trend Richtung Phänotyps des Wildtyps festgestellt werden, jedoch mit nicht-signifikanten Unterschieden. Dasselbe gilt für den Präsynapsenmarker α-synuclein. Geimpfte Tiere zeigen eine Verringerung der pathologischen Kennzeichen. Allgemein betrachtet konnten Verbesserungen der neuropathologischen Veränderungen in geimpften versus nicht geimpften transgenen Mäusen gezeigt werden.

Table of Contents

1 Introduction

1.1 Alzheimer's disease

Alzheimer's disease (AD) is the most common form of dementia. It is an incurable neurodegenerative disease affecting the elderly. The characteristic symptomatic hallmarks of AD are cognitive, behavioural and functional decline. The neuropathology is marked by formation of neuritic plaques composed of aggregated β-amyloid peptide, neurofibrillary tangles made up of hyperphosphorylated Tau protein and the early loss of neocortical synapses [1]. It is a progressive and terminal illness, but death of patients is caused by external factors due to continuous worsening of the physical and psychical state [2].

1.1.1 History of AD

AD was first described by Alois Alzheimer in his talk at the meeting of psychiatrists in 1906 [1]. He depicted the behavioural symptoms of his patient Auguste Deter. In the early stages of the disease, she lost her short-term memory and also her mood was changing fast from one extreme to the contrary. Later, also her long-term potentiation (LTP) was affected and Deter was not longer capable to manage daily life. After her death, Alzheimer examined Auguste Deter's brain by microscopy and different staining methods. He found a highly diminished brain mass, enlarged ventricles and protein deposits in the cortex. The congophilic deposits he named "amyloid plaques" and the fibrillar structures he entitled as "neurofibrillary tangles" [3]. All these behavioural and pathologic characteristics are still the standard of diagnosis of AD.

1.1.2 Incidence and diagnosis

Nowadays, the number of patients continuously rises, particularly in the industrial world where society is ageing. Worldwide more than 20 million people are affected by AD [4]. AD belongs to the most costly diseases in these parts of the world as in general long-term care is needed. In humans the pathology arises beyond the age of 70 [5], [6], except the early-onset hereditary form of the disease which even

starts around the age of 45-60 years [7]. The symptoms are characterized as in other dementias by the loss of memory and lowering of cognitive capabilities. Patients are strongly affected in their daily life. Especially in the advanced stage of the disease they are completely dependent on caregivers. The life expectancy in AD is decreased; however it is not possible to give each individual a general prediction at the time point of diagnosis as there are persons living decades with AD and others only a few years. On average death occurs 9 years after diagnosis [8]. The causes of death are external factors like downfalls, bedsores and pneumonia [2].
Until now, in the preclinical stage of AD there are no reliable symptoms established to make a confident diagnosis possible before the manifestation of irreversible damage of the brain. Cognitive tests can be carried out which give a certain probability of the existence of AD. However, this technique as well, is the more secure the further the disease is already progressed. Also the similarity to other forms of dementia makes it hard to diagnose AD. Often the disease is already advanced at the time point of a definitive diagnosis. This makes later treatment more difficult.

1.1.3 Genetic causes of AD

The pathogenesis of AD is not completely understood. It is predicted to be a interplay between different factors. Genetic aspects, life style, training of the brain memory function and ageing are important aspects in developing the disease. Estimations on the impact of familial AD defined through mutations in relevant genes, are diverging from about 0.1% of all AD patients [9] to 5-10% [10].
There are numerous point mutation sites known in the amyloid precursor protein (APP). Each substitution of an amino acid leads to an aberrant way of processing and deposition of the APP (see chapter 1.2). Protein aggregation and deposition of amyloid β (Aβ), a cleavage product of APP, result in so called senile plaques, which are predicted to be highly neurotoxic. In this context the elevated risk of developing AD in patients with chromosomal aberration should be mentioned. In the case of trisomy 21, the chromosome 21, on which the APP gene is located, is present in triplicate. This occurs by a non-disjunction event during meiosis. Hence, Aβ might be expressed at higher levels (the so called gene dosage effect) which can be the trigger for increased AD-like pathology development [4], [11], [12].
Presenilins are a family of transmembrane proteins and also seem to be involved in

AD pathogenesis. Presenilin 1 (PS1; also PSEN1) and PS2 function as subunits in the γ–secretase which is involved in processing events of the amyloid precursor protein. In some forms of the early-onset familial AD PS1/2 genes are mutated [5], [13].

Another genetic prevalence being discussed is one specific allele of the Apolipoprotein E (ApoE). The ApoE4 allele seems to be related with the late-onset and the sporadic form of AD [14]. Homozygotes for the ApoE4 allele show a higher prevalence for AD development than heterozygote ApoE4 carriers. Recent data imply that the probability to come down with AD is enhanced up to 90% in ApoE4 carriers compared to 20% in non ApoE4 carriers [15]. The mechanism how ApoE4 interferes with the progression of AD is not well understood. It can be assumed that ApoE4 plays a role in the formation of amyloidogenic plaques [13] and its clearance [16]. Proteolytically cleaved ApoE4 also seems to influence the phosphorylation of Tau protein [17].

Another protein involved in the pathology of AD is the highly soluble microtubuli associated protein Tau. It stabilizes microtubuli of neurons in the central nervous system, but it is rare in the rest of the body. Its hyperphosphorylation through different tyrosine or serine kinases leads to destabilization of microtubules and to aggregation of Tau. The so formed aggregates in neurons are called neurofibrillary tangles (NFTs) [4]. They are highly neurotoxic and responsible for synapse degeneration and neuron loss [18]. This is explained by the detachment of hyperphosphorylated and aggregated Tau from the microtubuli. This is followed by their breakdown, consequent failure in intracellular transport and neuron degeneration. The mutated human PS1 gene has been shown to be involved in Tau hyperphosphorylation [11]. Moreover, the presynaptic protein α-synuclein is believed to interact with Tau and thereby promotes its phosphorylation at specific amino acid residues [13], [19]. The complete role of the Tau protein in the pathogenesis of AD is not well understood, but there are several other neurodegenerative diseases, in which Tau is involved as well, e.g. FTDP-17, pick's disease, PSP [20].

1.2 The Amyloid Precursor Protein

The amyloid precursor protein (APP) is a conserved type I membrane protein. The

human APP gene is located on the long arm of chromosome 21. It is about 240kb long and made up of at least 18 exons [21]. The full length APP is 770 amino acids long and the polypeptides migrate between 110-140kD in gel electrophoresis [10]. There are three different major isoforms of the protein, APP695, APP751 and AP-P770 caused by alternative splicing. The longer variants contain a Kunitz-type ser-ine protease inhibitor domain, which is lacking in the shorter isoform. APP695 is predominantly expressed in neurons, whereas the other isoforms are ubiquitously expressed [22]. The whole protein consists of a small intracellular C-terminal do-main, a transmembrane region and a larger extracellular N-terminal domain. The protein is posttranslationally modified through glycosylation, phosphorylation and tyrosine sulphation. Its physiological function was unknown for a long time, but re-cently there is evidence for its involvement in synaptogenesis. APP is anterogradely transported targeting synapses the place in cells where it is active [12]. Its expres-sion is elevated during brain injuries and APP plays an essential role in neuronal migration as well as neuron plasticity. This could be shown among others by gener-ating an APP loss of function mutation in mice [21].

1.2.1 APP Processing

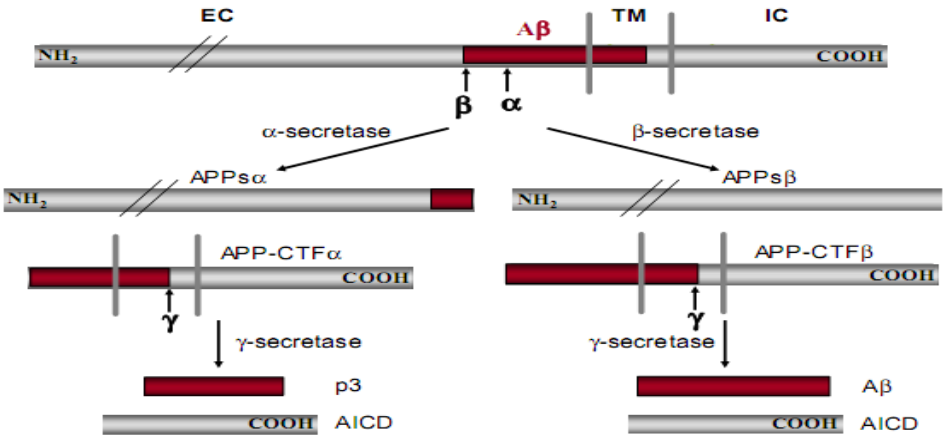

Figure 1: Schematic depiction of APP processing. EC: extracellular, TM: transmembrane, IC: intracellular, Aβ peptide is depicted in red (taken from Zheng and Koo, 2006)

Proteases of the secretase family are responsible for the different final products of APP. α- and β-secretases proteolytically cleave APP in the extracellular part (between aa 687 and 688 or 671 and 672, respectively); the γ–secretase, which is a

multiprotein complex including presenilins often being mutated in AD (see chapter 1.1.3), cleaves in the membrane-spanning domain (3 cleavage sites between aa 711 and 721) (Fig.1). Always two consecutive processing steps take place. The non-amyloidogenic pathway consists of a first cut by the α-secretase releasing sAPPα at the N-Terminus and APP-C-TerminalFragment(CTF)α. After this cleavage step the amyloidogenic processing is no longer permitted. The APP-CTFα is further processed by the γ–secretase resulting in the APP intracellular domain (AICD) and a 3kD small product, called p3. The pathological way of processing starts with a cut by the β-secretase (also known as BACE1 – β-site APP cleavage enzyme) resulting in the soluble APPβ and the APP-CTFβ. The latter cleavage product is further processed by the γ secretase releasing amyloid β and AICD [10]. In healthy people both ways of processing exist likewise [10].

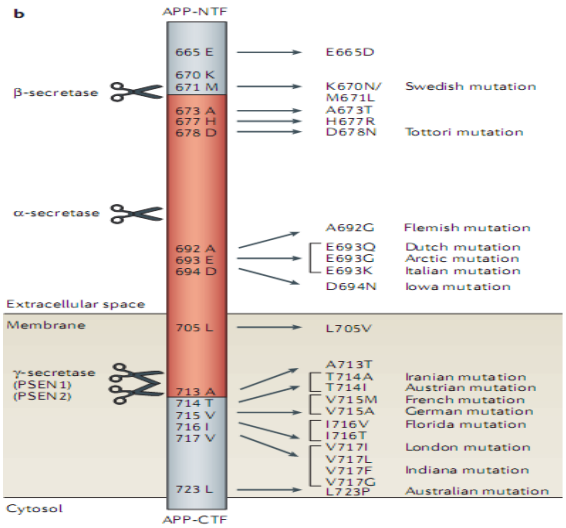

Figure 2: Part of the APP amino-acid sequence; mutations are highlighted; mutations are named after the nationality or location of the first family in which that specific mutation was demonstrated. Red: amyloid beta sequence. A, alanine; D, aspartic acid; E, glutamic acid; F,phenylalanine; G, glycine; H, histidine; I, isoleucine; K, lysine; L, leucine; M, methionine; N, asparagine; P, proline; Q, glutamine; R, arginine; S, serine; T, threonine; V, valine; Y, tyrosine. (taken from van Dam and De Deyn, 2006)

There are degradation (e.g. ubiquitination followed by proteasomal degradation) and clearing mechanisms of the amyloidogenic APP cleavage products, which do not work properly any longer in AD patients [16]. Hence, accumulation of abnormal processed fragments and their latter aggregation occurs. The conformation of Aβ from the soluble form into aggregates is a critical and not well understood mechan-

ism in AD [13]. However, it is known, that plaque formation also take place in brains of older intellectually normal persons not showing any dementia like symptoms [23]. Thus, the defect in processing is linked to ageing. Other linked aspects are mutations in the gene (Fig.2). Mostly, mutated sites are near the cleavage sites for secretases. Thus, altered processing followed by changes in the balance of the resulting products proceed [24].

1.2.2 Aβ

Aβ is a secreted, approximately 4kD small polypeptide derived from APP constituting the principle protein of senile plaques in AD [25]. Two kinds of soluble Aβ peptide are generated during APP processing: Aβ1-40 and Aβ1-42, depending on which cleavage site is used by the γ–secretase complex. The latter is less frequent (5-15% of total Aβ) [12], but shows more tendency to aggregate [10]. Therefore it is believed to act as a seed for the later neuritic plaque formation. This assumption can be explained as the two additional amino acid residues (namely isoleucine and alanine) of one Aβ42 peptide strongly bind to the amino acids 34 (leucine) and 35 (methionine) of another monomer. This leads to the characteristic β-sheet formation [26], [27].

1.2.3 sAPPα

It has been observed that APP expression is elevated during neuronal maturation and differentiation as well as in brain injury [21]. In these processes more of the secreted sAPPα (sAPPα) fragment is released which is believed to play an important role in the healing and regenerative process as a neuroprotective factor. It has been described that sAPPα mainly supports full-length APP in its function of neurite outgrowth [28], [29]. In addition there is evidence that sAPPα is involved in regulating stem cells. It stimulates the proliferation of EGF (epidermal growth factor) -responsive stem cells in the subventricular zone (acting as a cofactor for EGF). Moreover, sAPPα induces the differentiation of neuronal stem cells into the astrocytic cell lineage [12]. For all these events, sAPPα is necessary but not sufficient. Another known function of sAPPα is normalizing the calcium homeostasis in neurons which is protective against excitotoxycity [6].

1.2.4 The amyloid cascade hypothesis

The hypothesis was established to clarify the link between the abnormal accumulation of Aβ peptide and neurodegeneration in AD.

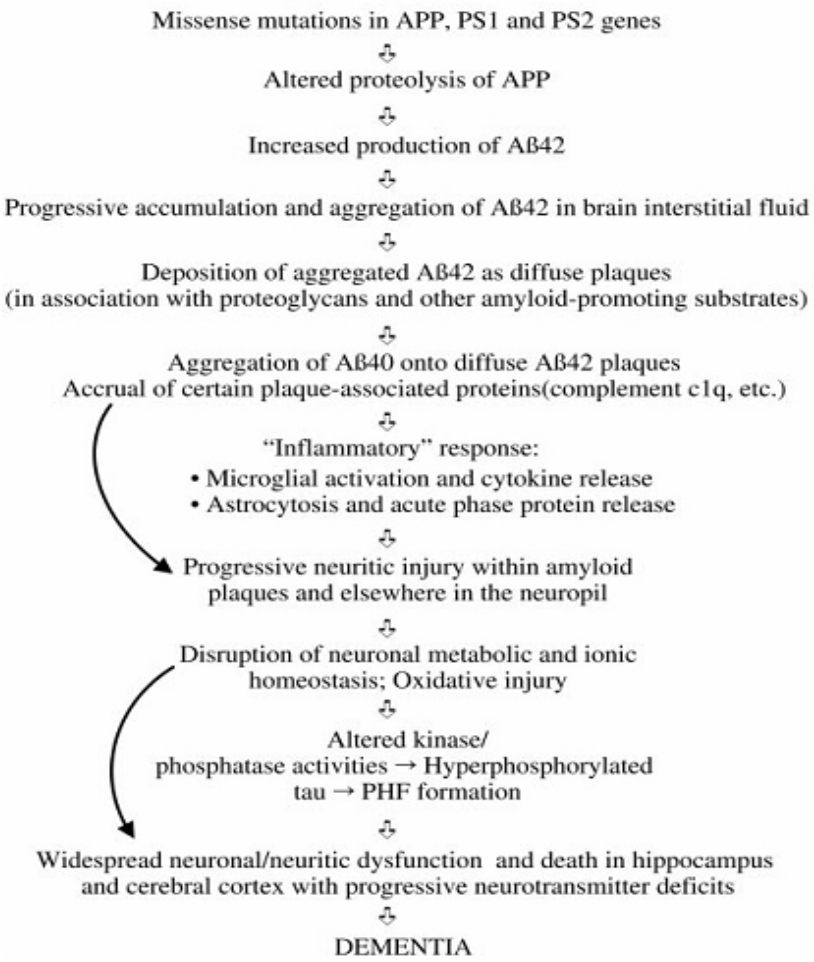

Figure 3: Scheme of a hypothetical progression of pathogenetic steps in familial forms of AD. For detailed description of the cascade see text. (taken from Selkoe, 2001)

The previously described soluble Aβ fragments are naturally produced. The hypothesis indicates that the abnormally increased concentrations of fibrilar Aβ42 compared to the soluble Aβ40 in AD favours the development of typical plaques. Monomeric Aβ42 form β-sheet structures, followed by protofibril- and fibrilformation [30]. Finally, they undergo dense aggregation and build up mature amyloid plaques [31]. Aβ40 is assumed to only co-deposit in the mature neuropathologic plaques [10]. The Aβ hypothesis states that the following neuropathologic damage that occur in

AD are all triggered by Aβ deposition. These include inflammatory responses, neuronal loss, hyperphosphorylation of Tau and many more (Fig.3).

Initially, the correlation between fibrilar Aβ and neurotoxicity has been demonstrated by application of synthetic Aβ monomers on neuronal cell cultures. The researchers found out, that only “matured” Aβ solution (allowed to aggregate during 3 day incubation) shows toxic properties, but not freshly applied Aβ monomers [32].

However, the hypothesis is disputed among scientists. Critical points are the partial correlation between the amount of neuritic plaques and the degree of dementia. Furthermore, as mentioned before (see chapter 1.2.1) also non-demented aged individuals show plaques. Besides high neuron loss could be shown in areas of the brain with no plaque load [32].

Another upcoming idea is the oligomer hypothesis which claims soluble Aβ42 oligomers to be the main cause of toxicity. This prediction was made in connection with an experiment in which Aβ fibril formation was inhibited resulting in increased cell toxicity. This phenomenon was explained by the shifted balance in favour of oligomeric Aβ [33].

1.3 Alterations in the neuronal network and AD associated pathologic alterations

In brains of AD patients neuropathologic alterations have been observed. All these findings are more or less associated with the presence of Aβ deposits or NFTs. Mostly, it is still under investigation which event or pathologic alteration in the pathogenesis of AD is the cause of or leads to other AD related phenomenons.

The first change in AD brains to be mentioned is the loss of neurons and synapses. Synapses are the place in the brain were transmission, processing and storage of information take place. Synapses exist between two neurons, thus building a huge interconnecting network. As the main cause of synaptic loss, death of neurons is mentioned [34]. Moreover, synapses of living neurons degrade in case that the connected synapses decease in consequence of dying neurons. It has been shown that synapses of living neurons containing NFTs are more susceptible to degeneration than those of non-NFT containing neurons [35]. The analysis of synaptic alterations is done by using common pre- and postsynaptic markers like α-synuclein and

PSD95. The breakdown of synapses leads to altered accumulation of these pre- and postsynaptic factors.

Equally, neurotransmitter levels can be analysed. Death of certain neurons, e.g. cholinergic neurons cause impairment in the concentrations and effectiveness of the transmitter acetylcholine.

Furthermore, dendritic markers can be used to highlight alterations in the structure of neurons and their branches in AD affected brains. One of these markers is MAP2, which is a microtubuli associated protein only present in dendrites but not in axons (Tau is the equivalent protein in axons). Other markers are Drebrin and ARC/Arg3.1. Both are expressed in dendritic spines. Spine plasticity is involved in motivation, learning and memory. Dendritic spines are highly flexible, although after LTP they can get very stable.

Cerebral amyloid angiopathy is a side effect of Aβ accumulation. Amyloid β deposition also takes place in blood vessels causing their weakening and occlusion. This, in further consequence, leads to cerebral microhemorrhages [36] and thus might cause stroke. CAA incidence varies with the APP mutation [16].

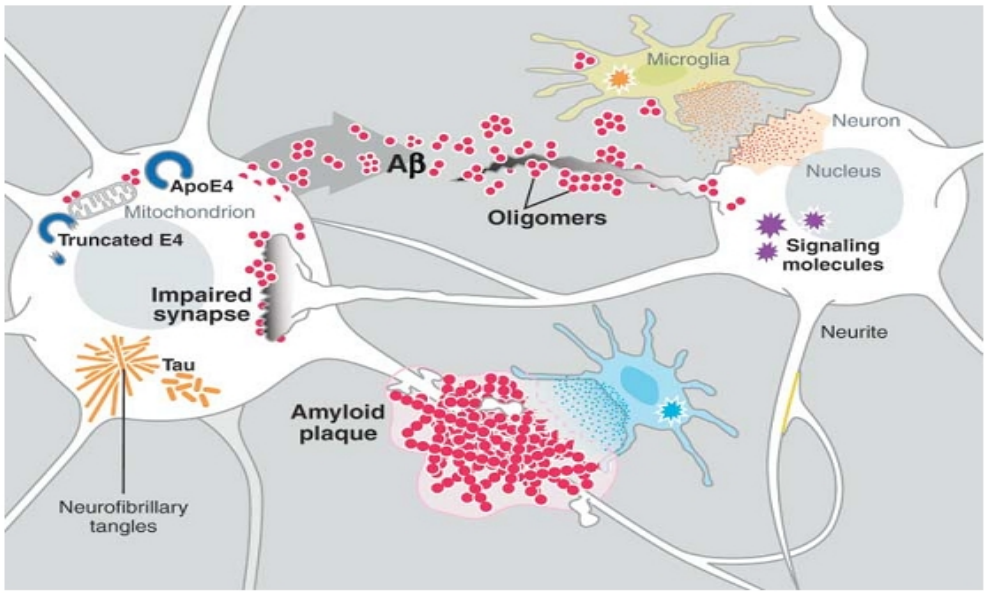

Figure 4: Summery of the impairments caused by pathogenic amyloid β assemblies. For details see text. (taken from Roberson and Mucke, 2006)

Another early pathological manifestation in AD is astrogliosis. It describes the increased accumulation of astrocytes. Astrocytes are responsible for supporting, pro-

tecting and nourishing neurons [4]. They are socialised within the plaques as they also fulfil their clearing function as immune cells of the central nervous system [4]. Microglia are also part of the immune system and responsible for inflammation at site with abnormal accumulation of proteins such as Aβ or Tau. What is meant to clear harmful agents can also cause damage to neuronal cells (for summary see Fig.4).

1.4 Therapeutic strategies against AD

Up to now there is no cure available for AD. There are medications like acetylcholine (ACh) esterase inhibitors and N-methyl D-aspartate receptor (NMDAR) agonists. The former is applied to counteract the loss of active acetylcholine caused by death of cholinergic neurons. This is mediated by inhibiting the enzyme ACh esterase which triggers the conversion of acetylcholine into the inactive metabolites acetate and choline [37], [38]. The second pharmaceutical blocks NMDA receptors. This prevents overstimulation through the excitatory neurotransmitter glutamate binding normally to the receptor. This would provoke excitotoxicity, which implies the damage of nerve cells by an increased influx of calcium ions [39]. These medications are used as symptomatic treatment. They are unable to halt or only to slow down the progress of AD. For long term treatment, a remaining promising and in the end very effective approach to fight this widespread disease, could be immunotherapy.

1.4.1 Active immunization against Aβ

The medical term “immunotherapy” can be defined as “treatment of a disease with therapeutic agents that promote or inhibit immune responses” [40].
Vaccination is one kind of immunotherapy. It can be distinguished between passive and active immunization as well as vaccination as prophylactic or therapeutic approach. Passive immunization in general implicates the direct injection of specific monoclonal antibodies into the person (or animal) to prevent or combat already existing diseases. This vaccination has to be repeated when the antibody titer in the blood stream decreases.
Active immunization consists of the appliance of an antigen, the vaccine, to evoke an immune response. For example, in the case of many viral infections attenuated

or killed virus particles were injected to provoke an immune response against the specific virus. In the case of a later infection with the virus, memory B-cells are able to produce high amount of the specific antibody and the infection can be cleared easily and rapidly by the adaptive immune system. The antigen is mostly coupled to an adjuvant to boost the immune response. Active immunization against Aβ has been shown to be quite complicated since the blood brain barrier has to be crossed by the induced antibodies. In a vaccination approach using the original full-length Aβ sequence, patients came down with meningoencephalitis in the clinical trial [4], [41]. It is now believed that this effect was due to a T-cell response since all affected patients showed CD4+ and CD8+ T-cell infiltrates in the brain [4].

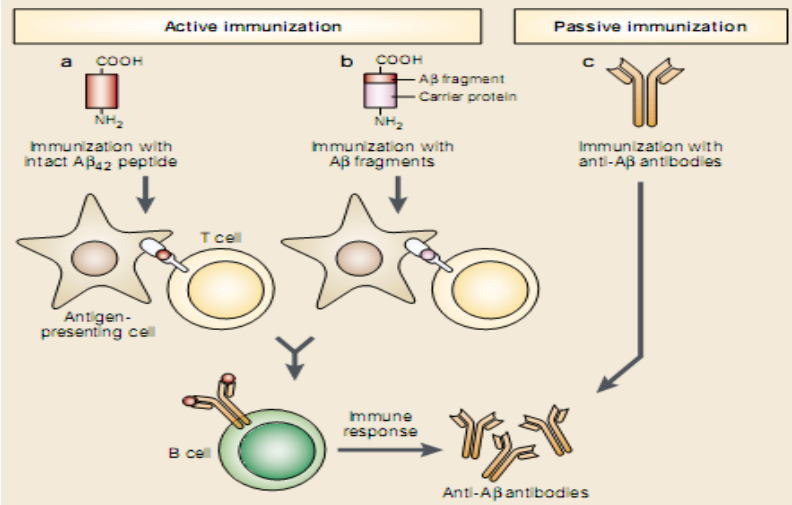

Figure 5: Schematic drawing of different vaccination approaches against Aβ. a)&b) active immunizations leading to Aβ-specific antibody production, a) full length Aβ42 peptide is used for immunization, b) an Aβ fragment is coupled to a carrier protein to stimulate required T-cell response, c) passive immunization by injecting anti-Aβ antibodies. (taken from Schenk, 2002)

Therefore AFFiRiS AG is developing a safer form of Aβ vaccine [42], [43]. AFFiRiS AG is aiming to develop secure active vaccines against different widespread diseases as atheriosclerosis, high blood pressure, Parkinson's disease (PD) and Alzheimer's Disease. The fundamental technology consists of short peptides called AFFITOPEs, which mimic parts of the amino acid sequence of the target molecule. This induces antibody production against the target protein by B-cell stimulation. Inflammation caused by (cytotoxic) T-cells is not provoked since the peptides are too

short to be recognized by them. T-helper cells releasing cytokines needed for B-cell maturation and generation of antibodies are stimulated by coupling the peptide for vaccination to a carrier protein and an adjuvant (Fig.5) [44], [40]. In the case of AD the peptide is mimicking the N-terminal region of the Aβ peptide.
In different preclinical studies it could be shown that in vaccinated Tg2576 mice the amount of both soluble and aggregational amyloidogenic Aβ is significantly decreased compared to non-vaccinated transgenic mice. In immunohistochemical investigations it has been shown, that the area of plaques and the overall plaque load in the vaccinated animals were lowered (Mandler et al., manuscript in preparation). In accordance to this, amelioration of the cognitive function could be determined in behavioural tests like the morris water maze. Since these results of the preclinical experiments in the animal model are quite promising, AFFiRiS AG already started the clinical trials.

1.5 The mouse model

The different occurring mutations in the APP as well as in PS1 and PS2 have been used to generate mouse models for AD. In this study the Tg2576 animal model has been examined. The mutant human amyloid precursor protein (APP) containing the double Swedish mutation (K670N, M671L) is brought into a 129S2 laboratory mouse strain. The transgene is under the control of the hamster prion promoter. This promoter allows preferential expression in the central nervous system [11] leading to highest accumulation of the transgene in the brain [31]. However, human APP expression is not confined to the brain, but can also be detected in other tissues like heart, skin, muscle and many more [31], [45]. The transgenic animals show 5 to 6 fold overexpression of APP compared to a wildtype non-transgenic animal [46]. The onset of formation of senile plaques with Congo Red-positive cores is about 7-8 months of age [31]. The most predominant form of Aβ present in Tg2576 is Aβ1-40 [31], [47], whereas this is only the case in 33% of AD patients [48]. Moreover, in Tg2576 only 5% of the Aβ is N-terminally truncated or modified, whereas in human AD brains this is the case in 69 -85% of insoluble Aβ [31]. In the water maze strong behavioural deficits of the animals could be observed [47], [49]. Compared to other models, these mice do not show a severe phenotype, but in

general, one can say that this animal model provides all the features for investigation of Aβ plaque formation. Tg2576 mice do not reflect all aspects of AD like for example hyperphosphorylated Tau protein that gives rise to neurofibrillary tangles. Thus, for research on Tau protein and its influence on AD, another mouse model has to be used.

1.6 Aim of the thesis

In addition to the reduction of plaque load and plaque area in the affected brain regions, active vaccination against Aβ should lead to an improvement of the neuronal functionality and integrity as well as an increase in the synaptic density. In this work some characteristic markers for these features were investigated in the Tg2576 mouse model. First, general comparisons of wildtype and transgenic animals were carried out by biochemical and immunohistochemical analysis. In the case of detectable pathologic alterations concerning protein concentrations or localisation in transgenic animals, vaccinated transgenic animal were analysed focusing on these AD associated pathologic hallmarks and their possible amelioration after active immunotherapy. Neurotransmitter levels as well as neuroprotective factor concentrations were measured by enzyme linked immunosorbent assay kits provided by different companies. Amounts of pre- and postsynaptic proteins in differently treated animals were compared using western blotting. Thus, homogenates of complete brain hemispheres were analysed. Immunohistochemistry was used to determine light alterations of certain markers in distinct brain regions. With this method also the pathological phenotype of neurons neighbouring the neurotoxic Aβ aggregates could be visualised.

2 Methods and Material

2.1 Genotyping PCR

Genomic DNA from mouse tail tips was used for genotyping PCR to detect the presence of the transgene. As internal control, primers for a housekeeping gene were used.

2.1.1 Digestion of mouse tail tips and Extraction of DNA

For genotyping mouse tail tips were used for genomic DNA purification (genomic DNA purification system; Promega). Mouse tail tips (2-3mm) were transferred into 1.5ml tubes. 275µl digestion solution were added to each sample and incubated over night (ON) at 55 °C. The next day, 250µl SV lysis buffer was added and vortexed. Mixture was transferred to minicolumns and spinned for 3min with 13000g. The flow-through was discarded, 650µl wash solution added to the column and centrifuged for 1min with 13000g. Washing was repeated for 3 times followed by centrifugation for 2min at 13000g. Then matrix was dried by 2min centrifugation with 13000 g. For elution, the columns were placed in new 1.5ml microcentrifuge tubes and 250µl nuclease-free water was added on the matrices. After 2min incubation the columns were centrifuged 1min with 13000g. This step was repeated once using the eluate from the previous step, to increase DNA concentration.

Digestion Solution Master Mix

	µL per reaction
Nuclei Lysis Solution	200
0.5 M EDTA (pH 8.0)	50
Proteinase K (20mg/mL) (Roche)	20
RNase A Solution (4mg/mL)	5
	275

2.1.2 Polymerase Chain Reaction (PCR)

In the polymerase chain reaction sequence specific primers bind to DNA and allow amplification by Taq polymerase (Promega 5u/µl). The transgene and one house-

keeping gene were enriched to identify the genotype of each animal.

Primers:

- Primermix for housekeeping gene

  APP-1: 5´- AAG CGG CCA AAG CCT GGA GGG TGG AAC A-3´

  APP-2: 5´- GTG GAT AAC CCC TCC CCC AGC CTA GAC CA-3´

- Primermix for APP transgene

  APP-2: 5´- GTG GAT AAC CCC TCC CCC AGC CTA GAC CA-3´

  APP-4: 5´- TGG ACG ATC TCC AGC CGT GGC ATT C-3´

Reagents used for one PCR reactions were mixed in 200µl thin wall PCR tubes:

PCR Mastermix	
	µl per reaction
Template DNA	1
10x reaction mix (Roche)	2,5
Taq polymerase	0,25
10mM dNTPs (Promega)	0,5
$MgCl_2$ (50 mM)	1
Forward primer	0,5
Reverse primer	0,5
MiliQ water	18,75
	25

Tubes were placed into Biometra T3 Thermocycler and the following PCR program was performed:

- 90°C for 2min. (DNA-denaturation step)
- PCR amplification: 35 cycles of:

  90°C for 15sec. (denaturation of basepairs)

  57°C for 30sec. (annealing of primers)

  72°C for 90sec. (elongation of primers)

- Final extension:

  72°C 5min.

  4°C hold

2.1.3 Gel electrophoresis

Gel electrophoresis was used to separate DNA in an agarose gel with respect to different size, thus the outcome of the PCR can be visualised. A 1.2% agarose gel was poured. Therefore 0.6g agarose (Invitrogen) were dissolved in 1xTAE by heating it up in the microwave. For detection of the nucleic acid the intercalating reagent SYBR safe (Invitrogen) was added to liquid agarose before the gel was casted. Samples for gel electrophoresis were mixed with loading buffer and separated by 10V/cm of the gel. DNA ladder used as standard was FastRuler DNA ladder low range (Fermentas). The UVP UV-Transilluminator was used for detection of DNA signals.

2.2 Histochemical Analysis

For all experiments Tg2576 respectively wt 129S2 mice were used. Mice were killed by decapitation. Blood was collected, brains were removed immediately and tail tips were used for genotyping. The blood samples were centrifuged at 10000rpm for 10min. The supernatants were stored at -20C° marked as sera. Brains were prepared for both histochemical and biochemical analysis. For the histochemistry one hemibrain was fixed in 4% paraformaldehyde, for the biochemical approach the other hemibrain was snapfrozen in liquid nitrogen and stored at -80°C until further use.

2.2.1 Brain fixation and dehydration

The hemibrains which have been used for histochemistry, were fixed and dehydrated to be further sectioned with the microtome. After over night (ON) incubation in 4% PFA (VWR) at 4°C, the following steps were performed:

1- Wash 30min in PBS
2- Incubate 2h in 30% EtOH (Merck) solution, then 1h in a fresh 30% EtOH solution
3- Incubate 2x2h in 50% EtOH solution
4- Incubate over the weekend in 70% EtOH solution
5- Incubate 30min in fresh 70% EtOH
6- Incubate 2x1,5h in 90% EtOH solution

7- Incubate 2x1,5h in absolute EtOH
8- Incubate 10min in Xylene (Roth) in glass beakers
9- Incubate ON in liquid Paraplast (Roth)(in open tubes – Xylene can evaporate)
10- Incubate in fresh liquid paraffin for 4h
11- Embed the hemibrains with the embedding molds and cassettes

2.2.2 Sectioning

Tissue sections of 7µm thickness were made with microtome (Leitz 1516) and placed on glass slides (ThermoScientific). Slides were dried at RT for at least one night before the sections were stained with different agents.

2.2.3 Deparaffinisation and Rehydration of Sections

For all staining procedures first the paraffin has to be removed from the sections and they have to be rehydrated. For this procedure slides were put into appropriate glass jars.

1- Xylene 1: 5min
2- Xylene 2: 5min
3- Ethanol Absolute: 5min
4- Ethanol Absolute: 2min
5- Ethanol 70%: 2min
6- Ethanol 50%: 2min
7- Ethanol 30%: 2min
8- ddH_2O

Steps 1, 2 and 3: under the fume hood!

2.2.4 Immunohistochemistry (IHC)

Immunohistochemistry benefits of the high affine binding between antibody and antigen. This interaction allows meticulous detection and distinction of different cell types or protein accumulations or alterations in certain areas of tissue sections. Bound antibodies were visualised through an enzymatic reaction which leads to colour development. This signal is amplified through the avidin-biotin complex.

Primary antibodies:

Ms monoclonal 3A5 (AFFiRiS AG) 1:1000

Ms monoclonal anti-NeuN (Millipore) 1:500

Rb polyclonal anti-GFAP (Chemicon, Millipore) 1:500

Secondary antibodies:

Goat anti-mouse IgG biot. (H+L) (Vector Labs) 1:250

Anti-rabbit IgG biot. (Vector Labs) 1:250

(All antibodies were diluted in protein concentrate (MOM Kit, Vector) in PBS)

After deparaffinisation and rehydration antigen retrieval (AR) was performed using pH9 and pH6, respectively. Therefore slides were put into a plastic jar filled with 250ml of pre-warmed (RT) AR solution (DAKO) (in case of double staining, the optimal AR for both antibodies has been ensured). They were heated in the microwave (3min with maximal power, 10min with 360W). After cooling down to RT, slides were washed with PBS (all washing steps were repeated twice). Endogenous peroxidase was blocked by 10min incubation at RT in 3% H_2O_2 (Merck) diluted in PBS. After the next washing step slides were blocked for 1h at RT in MOM blocking solution (MOM Kit, Vector Labs; 1 drop in 1.25ml of PBS) in a humidified chamber. Next, slides were washed and then incubated with the primary antibody in a humidified chamber over night at 4°C (in case of a double staining, both primary antibodies - arose in different species - were incubated together). On the following day sections were washed followed by incubation with biotinylated anti-primary antibody in a humidified chamber at RT for 30min. The ABC solution (Vector Labs; 1 drop of reagent A and one drop of reagent B in 2.5ml PBS) is prepared 30min in advance. It is applied on the slides for 30min at RT in a humidified chamber after two inserted washing steps. Then, slides were washed twice with PBS and once with ddH_2O. DAB solution (Vector Labs) is prepared (1 drop of Buffer Stock Solution, 2 drops of DAB Stock Solution and 1 drop of Hydrogen Peroxide Solution were well mixed in 2,5ml PBS) and applied on slides at RT for about 5min (depending on colour development, which was checked under the microscope regularly). Staining reaction is stopped with ddH_2O and sections were counterstained with hematoxylin (Sigma) for about 2min (colour is developed by rinsing slides in tap water).

(In the case of double staining, the counterstain was omitted. After DAB incubation slides were washed with ddH_2O and PSB, followed by 30min incubation with the other secondary antibody. The ABC step was repeated with the appertaining wash-

ing steps. As the substrate for this secondary antibody HistoGreen (Linaris) was used. Therefore 2 drops of HistoGreen Chromogen and 2 drops of H_2O_2 were properly mixed in 1ml HistoGreen buffer. The solution was supplied for 5min on the slides. Reaction was controlled permanently under the microscope and stopped with 1xPBST followed by ddH_2O. Sections were rapidly dehydrated in three times 30sec EtOH abs. and two times xylene for 30sec. Permanent embedding as usual)
Subsequently, brain sections were dehydrated:

1- Ethanol 30%: 2min
2- Ethanol 50%: 2min
3- Ethanol 70%: 2min
4- Ethanol abs: 2min (2x)
5- Xylene 2: 2min
6- Xylene 1: 2min

Steps 4, 5 and 6: under the fume hood

Slides were coverslipped with Entellan Neu Mounting Medium (Merck) and microscope cover glasses (ThermoScientific) for Mirax scanning (Zeiss).

2.2.5 Immunoflourescence staining (IF)

The method works in the same way as IHC only the visualisation differs. Flourophore-tagged antibodies were used and detected via illumination with light of a specific wavelength. The signal reflects the real amount of the molecule of interest.

Primary antibodies:

Ms monoclonal 3A5 (AFFiRiS AG) 1:200
Ms monoclonal anti-MAP2 (Millipore) 1:250
Ms monoclonal anti-NeuN (Millipore) 1:400
Rb anti-α-synuclein AB5038 (Chemicon, Millipore) 1:200

Secondary antibodies:

Fluorescein goat anti-mouse IgG (H+L) (Vector Labs) 1:100
Texas Red goat anti-rabbit IgG (H+L) (Vector Labs) 1:100
Fluorescein goat anti-rabbit IgG (H+L) (Vector Labs) 1:100

(All antibodies were diluted in 4% normal goat serum in 1xPBST)

The protocol of DAB staining is performed until sections were cooled down to RT after AR, beside the fact that for all washing steps 1xPBST was used instead of 1x-PBS. Then, slides were directly put in blocking solution (4% NGS in 1xPBST) for 1h at RT. Incubation with first antibody follows, ON at 4°C (in the case of double staining, primary antibodies – gained of different species - were incubated together). The next day, sections were washed and incubated with the secondary antibody for 30min at RT (double staining: both primary antibodies were incubated together). After two following washing step, slides were washed for 5min in ddH_2O. Finally, slides were coverslipped with vectashield mounting medium containing DAPI (Vector Labs). The next day dried slides were scanned with Mirax Scan (Zeiss). They were stored in the dark at 4°C.

2.2.6 Congo Red (CR) Staining

Staining Solutions

NaCl Stock Solution sat.

30g NaCl (VWR) and 200ml ddH_2O were well mixed, addition of 800ml EtOH abs.

NaCl Working Solution

50ml NaCl Stock Solution, 0.5ml 1% NaOH (Merck)

Congo Red Stock Solution, sat.

1g Congo Red Powder (Sigma) and 500ml NaCl Stock Solution were well mixed

Congo Red Working Solution

50ml Congo Red Stock Solution, 0.5ml 1%NaOH

As this staining method always was used in combination with immunofluorescent stainings, sections were rehydrated as usual. Also the AR and two following washing steps with PBST were performed. Then, slides were placed into freshly prepared NaCl Working Solution for 20min followed by 1h incubation in freshly filtered (whatman filter, VWR) Congo Red Working Solution. Slides were washed with PBST twice. Afterwards the normal IF protocol was followed (see above).

2.2.7 Image Analysis using Fiji software (version fiji-win32-20100614)

For image analysis Fiji software program (version fiji-win32-20100614) in combination

with MIRAX viewer has been used. For detailed description of evaluation protocol see chapter 3 at the appropriate sections.

2.3 Biochemical Analysis

2.3.1 Extraction of murine brain tissue

Buffers required:

Homogenisation buffer I (HBI) for 20 mL: 1mL 1M HEPES (Sigma) (pH 7.3), 0.2mL 0.5M EDTA (Sigma), 18.8mL ddH_2O and 2 protease inhibitor (PI) cocktail tablets (complete mini)(Roche)

Homogenisation buffer II (HBII) for 20mL: 9.56g of Guanidin-HCl (Roth) were dissolved in 13mL ddH_2O, addition of 1mL of 1M HEPES (pH 7.3), 0.2mL of 0.5M EDTA and 2 PI cocktail tablets (complete mini)

Dilution buffer for 80mL: 2mL of ice-cold 1M HEPES (pH 7.3), 50µL of 0.5M EDTA and 8 PI cocktail tablets (complete mini), the volume was filled to 80mL with ddH_2O

1- Each hemibrain and muscle was homogenised in 1mL of ice-cold HBI using a douncer. Samples were always kept on ice and foaming of suspension was avoided. Homogenates were transferred into an ultracentrifuge-extra-safe 1.5mL tube and stored at -80°C until further processing.
2- Then homogenates were ultracentrifuged at 4°C and 40000 rpm for 30min. Supernatant was aliquoted and stored at -80°C as soluble fraction.
3- Pellet was resuspended in 1mL of HBII and incubated 3h at 4°C with constant rotation. The resulting suspension was diluted in 4mL of ice-cold dilution buffer and then centrifuged at 4°C and 13000rpm for 20min. The supernatant was aliquoted and stored at -80°C as insoluble fraction. The pellet was discarded.

2.3.2 Dialysis of brain insoluble fractions

Dialysis cassettes (10000MWCO; ThermoScientific) were washed for at least 10min in ddH_2O. Insoluble brain samples were carefully transferred into dialysis membranes using a syringe and dialysed against 5L of PBS for 1h at RT with slow agitation. For ON dialysis samples were transferred in new cold buffer at 4°C. The

next day membranes were transferred into fresh PBS (5L) again and dialysed three more hours at 4°C. Dialysed homogenates were transferred into a 1,5ml plastic tube and stored at -80°C marked as dialysed insoluble fraction.

2.3.3 Enzyme Linked ImmunoSorbent Assay (ELISA)

6 different ELISA Kits have been used to determine the amount of three different neurotransmitters, a neuroprotective factor and one protein in mouse brain homogenates:

2.3.3.1 Serotonin ELISA (IBL international)

The assay follows the principle of a competitive ELISA whereby biotinylated and non-biot. antibody compete for the immobilized antibody binding sites. The OD at 405nm (reference wavelength: 600-650nm) was measured and the serotonin content (ng/ml) has be calculated via the 4-parameter program (Tecan Sunrise reader).
Standard provided: 0.0 ng/ml, 0.08 ng/ml, 0.24 ng/ml, 0.73 ng/ml, 2.2 ng/ml, 6.6 ng/ml, 19.8 ng/ml
Procedure:
Samples and provided controls were acylated before ELISA procedure. Therefore 20µl of the brain homogenates and controls were mixed with assay buffer and acylation reagent and incubated (15min, 37°C). For this purpose disposable glass centrifuge tubes (Corning) has been used. Subsequently 2ml assay buffer was added and the mixture was centrifuged for 10min at 1500g.
50ml of the supernatant of acylated samples and controls were pipetted into the appropriate wells of the microtiter plate. Serotonin Biotin and serotonin Antiserum were added and covered plate was incubated for 90min at RT on an orbital shaker (500rpm). After properly washing the wells with provided washing buffer, enzyme conjugate was added, followed by further incubation for 60min (same conditions). Next, after another washing step, substrate solution was added; incubation 60min (same conditions). The reaction was stopped by the addition of stop solution and OD was measured.

2.3.3.2 Dopamine ELISA (IBL international)

This assay is based on the principle of a sandwich ELISA. The microtiter plate is

precoated with goat anti-rabbit antibodies. The antigen in the samples and controls were captured by a liquid antibody, which binds to the coated antibody. Detection occurs via an enzyme-coupled second antibody binding sites. The signal produced by the substrate is proportional to the Dopamine amount in the sample. The OD is measured at 405nm (reference wavelength: 600-650nm) and the dopamine content (ng/ml) has be calculated via the 4-parameter, cubic spline and LogitLog program (Tecan Sunrise reader).

Standard provided: 0.0 ng/ml, 60 ng/ml, 180 ng/ml, 585 ng/ml, 2300 ng/ml, 11470 ng/ml

Procedure:

Samples, supplied controls and standards were extracted before ELISA procedure. Therefore 50µl or 100µl of the brain homogenates and 20µl of standards and controls were mixed with extraction buffer and incubated (30min, RT, 800rpm) in provided extraction plates. Subsequently, wells were washed with ddH_2O 5min on the shaker. Then, extraction buffer and acylation reagent were added and extracted 20min (RT, 500rpm). After another washing step, incubation with release buffer followed (30min, RT 500rpm). The resulting samples were diluted in release buffer 1:51.

75ml of freshly prepared COMT Enzyme Solution were applied into each well. 100µl of the diluted extracted samples and controls were added as well as 50µl Dopamine Antiserum. The covered plate was incubated for 120min at RT on an orbital shaker (500rpm). After properly washing the wells with provided washing buffer, enzyme conjugate was added, followed by further incubation for 60min (same conditions). Next, after another washing step, substrate solution was added; incubation 40min (same conditions). The reaction was stopped by the addition of stop solution and OD was measured.

2.3.3.3 Mouse acetylcholine (ACH) ELISA Kit (Cusabio Biotech co., Ltd)

This kit is based on the principle of a sandwich ELISAs (see above). TMB is used as substrate for the horse radish peroxidase and the signal obtained is proportional to the quantity of murine ACh in the brain homogenates.

Standard provided: 0.15 ng/ml, 0.312 ng/ml, 0.625 ng/ml, 1.25 ng/ml, 2.5 ng/ml, 5

ng/ml, 10 ng/ml

Procedure:

100µl of diluted (1:5) samples, standards and blanks were pipetted as duplicates into precoated wells of the microtiter plate. After incubation for 2 hours at 37°C, 100µl of the biotin-labelled antibody was added and incubated for one more hour at 37°C. After washing the wells, HRP-avidin working solution was added; incubation for 1h at 37°C. Subsequently, another washing step was performed before TMB substrate was applied for 10-30min at 37°C depending on colour development. Reaction was stopped with stop solution and the OD was measured at 450nm wavelength with Tecan ELISA reader and the adequate program of Magellan was used to obtain a standard curve and the corresponding equation. Thus, concentrations of the protein of interest can be determined in samples.

2.3.3.4 Human sAPPα (highly sensitive) Assay Kit (IBL international)

Both sAPPα kits are sandwich ELISAs (see above). TMB is used as Chromogen and the obtained signal is proportional to the quantities of human/murine sAPPα in the samples.

Standard provided: 0.78 ng/ml, 1.56 ng/ml, 3.13 ng/ml, 6.25 ng/ml, 12.5 ng/ml, 25 ng/ml, 50 ng/ml

Procedure:

100µl of diluted (1:100 for both assays) samples, standards and blanks were pipetted as duplicates into precoated wells of the microtiter plate. After incubation over night at 4°C, plate was washed. Then the labelled antibody was added and incubated for 30min at 4°C. The plate was washed again and the substrate was added; incubation for 30min in the dark at RT. Reaction was stopped with stop solution and the OD was measured at 450nm wavelength with Tecan ELISA reader and the adequate program of Magellan was used to obtain a standard curve and the corresponding equation. Thus, concentrations of the protein of interest can be determined in samples.

2.3.3.5 Mouse/Rat sAPPα (highly sensitive) Assay Kit (IBL international)

Standard provided: 10 pg/ml, 20 pg/ml, 40 pg/ml, 80 pg/ml, 160 pg/ml, 320 pg/ml,

640 pg/ml
Same principal and procedure as in 2.3.3.4.

2.3.3.6 ELISA Kit for Mouse Microtubuli Associated Protein 2 (MAP2) (Uscn Life Science Inc. Wuhan)

This assay is based on the principle of a sandwich ELISA. The microtiter plate is precoated with a MAP2 specific antibody which captures the antigen in the samples and controls. Detection occurs via an enzyme-coupled second antibody. The signal produced by the added substrate is proportional to the MAP2 concentration in the samples. The OD is measured at 450nm and the MAP2 content (ng/ml) has be calculated via the 4-parameter program (Tecan Sunrise reader).
Standard provided: 0.15 ng/ml, 0.312 ng/ml, 0.625 ng/ml, 1.25 ng/ml, 2.5 ng/ml, 5 ng/ml, 10 ng/ml
Procedure:
100µl of diluted (1:20) samples, standards and blanks were pipetted as duplicates into precoated wells of the microtiter plate. After incubation for 2 hours at 37°C, 100µl of detection reagent A working solution was added and incubated for one more hour at 37°C. After properly washing the wells, 100µl of detection reagent B working solution was added; incubation for 30min at 37°C. Subsequently, another washing step was performed before the substrate solution was applied for 15-25min at 37°C. Reaction was stopped with stop solution and the OD was measured at 450nm wavelength with Tecan ELISA reader immediately.

2.3.4 Western Blotting

Also in the western blot technique the binding between antigen and antibody is utilised. Proteins were separated according to their molecular weight in the electrophoresis. The protein of interest further can be easily identified by the incubation with the specific antibody and the following application of the HRP-labelled secondary antibody. The signal can be visualised by luminescence.

2.3.4.1 Bradford protein assay

Determination of protein concentration in a homogenate was done by Bradford assay. The dye reagent changes from red to blue by cationic and hydrophobic protein

binding with an absorbance maximum at 595 nm wavelengths.

For analysis the dye reagent concentrate (BioRad) was diluted 1:5 with ddH2O and filtered (whatman filter, VWR) to remove precipitates. BSA (2mg/ml; Pierce) serial dilutions were used as a standard (concentrations see below). Samples were diluted 1:8 (insoluble fractions) and 1:40 (soluble fractions) and used in duplicates. 10µl BSA standard or protein samples were pipetted on micotiterplates (Nunc) and 200 µl dye reagent was added and mixed. Plates were incubated at RT for 5min and then absorbance was measured at 595 nm wavelength with a plate reader (Tecan Sunrise).

Standard concentrations: 0.50mg/ml, 0.40mg/ml, 0.30mg/ml, 0.20mg/ml, 0.10mg/ml, 0.05mg/ml (pure ddH_2O is measured as blank)

2.3.4.2 SDS polyacrylamide gelelectrophoresis (SDS PAGE)

For the separation of proteins a polyacrylamide gel containing SDS was used, separating the molecules according to their molecular size.

For analysis a 4% acrylamide stacking gel and 10% (for proteins of MW between 30-120kD) or 12% (for proteins smaller than 30kD) acrylamide running gel were poured. For MAP2 Western Blotting 4-12% gradient gels from NuPAGE were used. The gradient allows separation of proteins from ~40kD (β-actin) to 250kD (MAP2).

Homogenized brain samples (soluble and dialysed insoluble fractions; dialysis protocol see above) were diluted with ddH_2O and mixed with sample buffer. Then proteins were denaturated at 90°C for 5min. 20µg total protein (determined by Bradford Assay, see above) were loaded on the SDS gel. 5µl protein ladder (PageRuler Plus prestained Protein Ladder, Fermentas) was loaded on each gel to indicate the size. Electrophoresis was performed in the gel chamber (Biorad, MGV-202) filled with 1x running buffer; 1x MOPS running buffer (NuPAGE) for gradient gels. 15mA per gel were applied (Power supply - Biorad, Power Pac). Gel run was stopped when front line moved far enough.

2.3.4.3 Western Blot

Primary antibodies:

Ms monoclonal anti-PSD95 (abcam) 1:1000

Ms monoclonal anti-Drebrin (abcam) 1:800

Ms monoclonal anti-MAP2 (Millipore) 1:4000

Rb polyclonal anti-α-synuclein AB5038 (Chemicon, Millipore) 1:2000

Rb polyclonal anti-ARC/Arg3.1 (Acris) 1:1000

Rb polyclonal anti-β actin (Novus Biologicals) 1:2000

Secondary antibodies:

Goat anti-mouse HRP IgG+IgM (H+L) (Jackson) 1:20000

Goat anti-rabbit IgG $F(ab)_2$-HRP (Jackson) 1:20000

(All antibodies were diluted in 5% milk powder in PBST)

The samples were separated by SDS gel electrophoresis according to molecular size. Then proteins got transferred voltage-dependent on a 0.2µm pore-size nitrocellulose transfer membrane (Sigma) For the blotting, sponges, whatmanpapers and membranes were soaked in 1x transfer buffer. A sandwich, sponge – filter paper – gel – membrane – filter paper – sponge was assembled. Western Blotting was performed in transfer buffer for 45min with 100V (keep cool!) or ON at 4°C with 15V constant. (Blot chamber – Mini Trans-Blot cell, Biorad).

Thereafter, membrane was stained with Ponceau S which binds to proteins. Thus, complete protein transfer to the membrane can be confirmed. The membrane was used directly for further experiments or stored at 4°C until further use.

Membrane was washed in PBST and blocked 1 hour with 5% (w/v) milk in PBST (alternatively blocking was done ON at 4°C). Then the membrane was incubated with the primary antibody diluted in 5% milk/PBST for 1 hour at RT or ON at 4°C followed by 3 times 10min washing with PBST to remove unspecific binding of the antibody. After that, membrane was incubated with the HRP conjugated secondary antibody diluted in 5% milk/PBST for 30min at RT and washed two times 10min with PBST and once 5min with PBS. ECL+ detection kit (GE Healthcare) was used for antibody detection. Signal was evaluated with UVP Bioimaging system.

After evaluation, the membrane can be stripped and used for another antibody incubation (protocol see below).

2.3.4.4 Membrane Stripping

Membrane was incubated for 30min at 50°C with the stripping buffer in a 50mL tube

followed by three washing steps with PBST each 10min. Then the standard WB protocol can be continued beginning at the blocking step.

2.3.4.5 Evaluation of WB with fiji-win32 (version fiji-win32-20100614) software

One fixed rectangle was laid over each single band on one blot. Next, the program measures the intensity of the bands in the chosen rectangles and shows them as peaks. Under these peaks manually the background levels have to be drawn for the calculation of the peak area. The obtained values for the certain protein band were divided by the values measured for the corresponding loading control band (in our case β-actin). Thus, the intensities of the bands are all normalized to the blotted amount of protein and can be compared (also blots among each other) in further analysis.

2.4 Buffers and solutions:

10x PBS (5 litres)

10g	KCl (Sigma)
10g	KH_2PO_4 (Merck)
57.5g	Na_2HPO_4 (Sigma)
400g	NaCl (VWR)

pH 7.4-7.6

1x PBST (1liter)

100ml	10x PBS
1ml	Tween20 (Roth)
900ml	ddH_2O

Agarose Gel

50 x TAE: (1 litre)

242g	TRIS (Roth)
57.1ml	Acetic acid (Roth)
100ml	0,5 M EDTA (pH 8,0) (Roth)

6x Loading Buffer

10mM	Tris-HCL (pH 7,6) (Sigma)
0.15%	Orange G (Sigma)
0.03%	Xylene Cyanol (Sigma)
60%	Glycerol (Roth)
60mM	EDTA (pH 8,0) (Sigma)

SDS-PAGE and WB

5x Sample Buffer

10%w/v	SDS (Fluka)
10mM	β-mercaptoethanol (Sigma)
20%v/v	Glycerol (Roth)
0.2M	Tris-HCl, pH 6.8 (Sigma)
0.05% (w/v)	Bromophenolblue (Sigma)

10% Running Gel

ddH_2O (Millipore)	12.300 ml
1.5M Tris-HCl, pH 8.8 (Sigma)	7.500 ml
10% (w/v) SDS (Fluka)	0.300 ml
30% Acrylamide (Roth)	9.900 ml
10% (w/v) ammonium persulphate (APS) (Roth)	0.150 ml
TEMED (Roth)	0.020 ml

12% Running Gel

ddH_2O	10.200 ml
1.5 M Tris-HCl, pH 8.8	7.500 ml
10% (w/v) SDS	0.300 ml
30% Acrylamide	12.000 ml
10% (w/v) APS	0.150 ml
TEMED	0.020 ml

4% Stacking Gel

ddH_2O	3.075 ml

0.5M Tris-HCl, pH 6.8	1.250 ml
10% (w/v) SDS	0.050 ml
30% Acrylamide	0.670 ml
10% (w/v) APS	0.025 ml
TEMED	0.005 ml

1x Running Buffer (1 litre)

3.03g	Tris-HCl (Sigma)
14.4g	Glycine (VWR)
1g	SDS (Fluka)

10x Transfer Buffer (1 litre)

30.3g	Trizma base (= 0.25 M) (Roth)
144g	Glycine (= 1.92 M) (VWR)

1x Transfer Buffer (2 litres)

400ml	Methanol (Roth)
200ml	10x transfer buffer
1400ml	ddH_2O

Stripping Buffer

20mL	10%SDS,
12.5mL	0,5M Tris HCl pH6,8,
0.8mL	β-mercaptoethanol
67.5mL	ddH_2O

3 Results

The transgenic mouse model Tg2576 for Alzheimer's disease has been examined regarding to alterations in the central nervous system apart from already well studied neuritic plaques.

3.1 Regenotyping

Initial genotyping has already been performed directly after birth of the mice. Regenotyping has been done after killing the mice to confirm and to clearly identify the transgenic and wildtype animals for further studies. The animals were regenotyped by extraction of DNA from tail tips. The PCR product was loaded on a 1,2% agarose gel to visualise the outcome (Fig.6). Per animal two different PCRs were performed. One with the primer pair specific for the transgene (b), the other with primers for a housekeeping gene (a). As controls, DNA samples of animals with known genotype were used. A water sample was used to prove the purity of the PCR (not shown).

Figure 6: Exemplary outcome and interpretation of genotyping PCR on a 1.2% agarose gel. a: primer mix A for the housekeeping gene; b: primer mix B for the APP transgene; nc: negative control; pc: positive control.

The figure just exemplifies some results. Of course, genotyping has been proceeded for all animals of all experiments.

3.2 Measurement of human and murine sAPPα levels with ELISA Kit in two different experiments

Secreted APP fragments, especially sAPPα, are predicted to be neuroprotective as it is involved in initial neurogenesis and after injuries. To guarantee the quality of the vaccine it is important to show, that the induced antibodies do not crossreact

with sAPPα. Especially, it is important that the vaccination has no negative influence on mouse sAPPα concentrations. On the other hand, it would be an advantageous impact of the vaccine when it leads to a rise of sAPPα in vaccinated animals compared to untreated transgenic animals.

First we compared tg with wt brain lysates regarding their sAPPα levels.

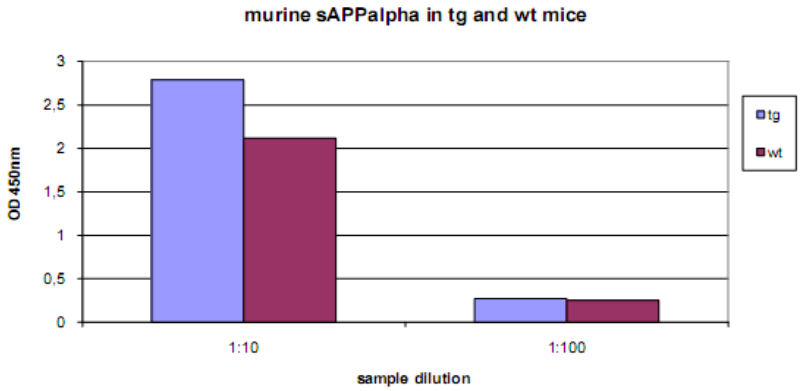

Figure 7: Optical density (OD) of murine sAPPalpha measured by ELISA in mice brain homogenates. The same samples were analysed applying two different dilutions. tg: transgenic; wt: wildtype

We were able to measure human (data not shown) and murine sAPPα levels in the brain homogenates (Fig.7). Interestingly, we found more of the neurotrophic APP metabolite in tg animals. Since only single samples have been measured, no statistics were done.

Further analysis of the neuroprotective factor sAPPα comprised two different experiments. Brain homogenates of differently vaccinated tg animals and control animals (PBS treated tg animals) involved in crucial preclinical experiments were investigated. The first experiment is a prophylactic vaccination approach in younger animals (first vaccination at the age of 6 months; Aβ accumulation just starts at the beginning of the vaccination). The second one is a therapeutic approach in older animals (first vaccination at the age of 12 months; Aβ deposition is already eminent at this time-point). In both groups, animals were vaccinated 6 times in monthly intervals and then sacrificed. Group 1 of both experiment includes control animals that were treated with PBS+Alum (aluminium hydroxide). Alum is an adjuvant contributing to a good Th2 antibody response. KLH (Keyhole limpet hemocyanin) is used as carrier, on which every peptide for vaccination usage is coupled. KLH is needed to

induce immunogenicity. After coupling to KLH,the peptide is mixed with Alum. Animals of group 2 of both experiments were vaccinated with the AFFITOPE AD03-+Alum and mice of group 5 of MV0408 were treated with the original Aβ1-6 peptide-+Alum (see table below).

	MV0208	MV0408
Age of animals	14 months	18 months
Vaccination approach	Prophylactic	Therapeutic
Number of groups	2	3
N° of untreated animals	9	9
N° of AFFITOPE/ Aβ1-6 vaccinated animals	10	7/7

Both the human as well as the murine sAPPα were measured with the appropriate ELISA Kits (IBL, Germany). Since the standards provided have different concentrations, the results are demonstrated independently with different scale bars (Fig.8).
All ELISA results were depicted in ratio to the wet weight (ww) of the hemibrain, determined immediately after brain preparation. In no group of both experiments statistically significant differences were detectable. That applies for both, murine and human sAPPα. Thus, we can conclude that at least no worsening in the sAPPα treshold is caused by vaccination. Of particular importance is, that the murine sAPPα concentrations in vaccinated animals are not reduced as this could indicate a harmful reaction of the induced antibodies versus the host.
For better visualisation of the positive effects of active immunotherapy against Aβ, also the Aβ loads of the investigated groups were shown (data taken from Mandler et al., manuscript in preparation; MV0408 group 5 has not been examined). This results were obtained by doing immunoflourescence staining on brain sections with the mouse monoclonal anti-Aβ antibody 3A5 (AFFiRiS AG). Briefly, the staining procedure was performed as described in chapter 2.2.5 (pH 9 for AR). Slides were scanned with Mirax Scan (Zeiss) and calculations of plaque load were done using Mirax Viewer and Definiens Software.
The results of the Aβ load show remarkable decline of the Aβ positive stained area in both experiments. In the therapeutic approach total plaque area was shown to be 36% decreased compared to the transgenic non-treated PBS group; in the prophy-

lactic approach the Aβ clearing efficacy is even higher (42%). This underlines the capability of the AFFITOPE vaccination to remove Aβ peptide from the brain.

Concluding, no negative effects on sAPPα of active immunization against Aβ can be deduced.

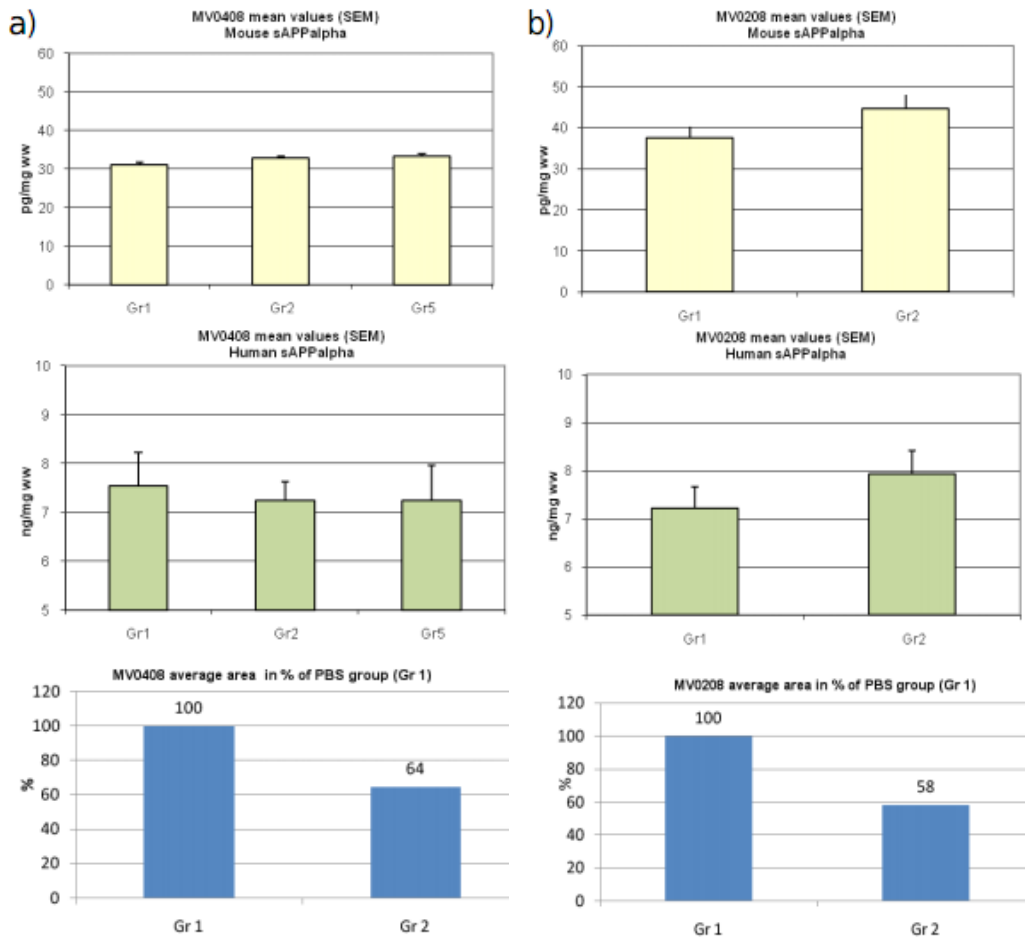

Figure 8: Human and murine sAPPα concentrations measured by ELISA in mouse brain homogenates. a) experiment MV0408, therapeutic approach; b) experiment MV0208, prophylactic approach. Additional, mean Aβ positive stained areas were shown for both experiments (Gr5 of MV0408 has not been examined). Gr 1: PBS+Alum; Gr 2: AD03+Alum; Gr 5: Aβ1-6 +Alum; SEM: standard error of the mean

3.3 Determination of neurotransmitter concentrations in wt and tg animals using ELISA

Next, we focused on Neurotransmitters. These endogenous chemicals are involved in the signal transmission at chemical synapses. They are stored in synaptic vesicles. Neurotransmitters were released into the synaptic gap after the arrival of an

action potential. At the postsynapse they bind on their specific receptors and are recycled or inactivated by different mechanisms. In AD patients a reduction of certain neurotransmitters is reported [50], [51]. Thus, we compared three different transmitter types in wildtype and transgenic animals by ELISA.

3.3.1 Serotonin

In humans, altered serotonin concentrations are associated with pathologic conditions such as schizophrenia, depression, chronic tension headache and hypertension. In AD patients decreased serotonin amounts were found. This is believed to be caused by the death of serotonergic neurons [50].

With the provided Kit (IBL, Germany) we were able to detect serotonin in the soluble fraction of mouse brain homogenates. The OD values of the samples were in the middle of the standard curve (between 3 and 5 out of 7 standards measured). Samples of wt and tg animals of different age were analysed. The mean data are shown in the diagram below (Fig.9).

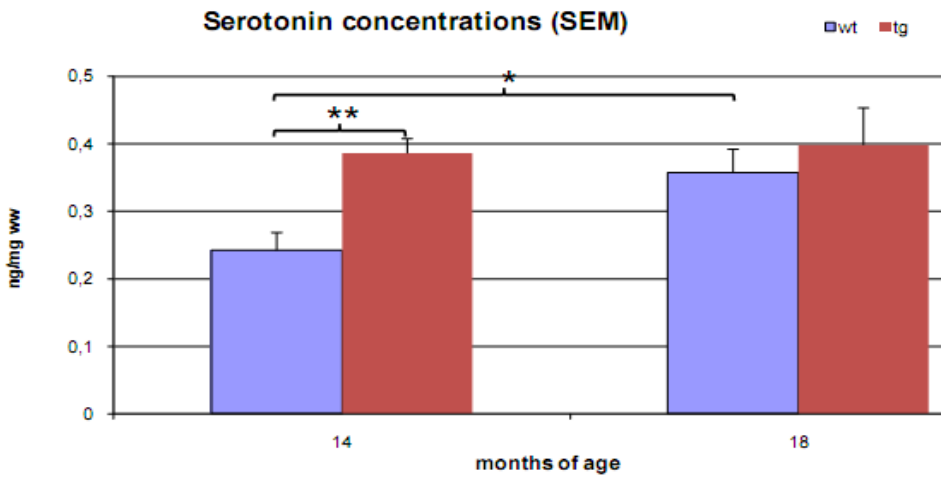

Figure 9: Serotonin concentrations in mouse brain homogenates. Measure by ELISA. wt: wildtype, tg: transgenic, 14: 14 months of age, 18: 18 months of age, SEM: standard error of the mean, * - significant (p<0,05), ** - highly significant (p<0,005)

Wt and tg animals at the age of 14 months show a significant difference (for wt/tg14: t-test, p=0,003, n=5; wt14/18: t-test, p=0,030, n=5). The older animals do not show any difference in the serotonin concentrations. They are quite comparable to the value of the younger tg animals. One must note that the number of animals measured per group is very small (5) and the standard deviation relatively high.

Thus, to prove significance larger groups of animals have to be analysed. Otherwise the 14 months old wt also can be seen as an outlier as all remaining groups show similar serotonin levels.
In the literature, serotonin is quantified as about 805ng/g of brain wet weight [52]. Our results reflect half the amount. The researchers used high performance liquid chromatography with electrochemical detection (HPLC-ECD) for their measurements. Therefore, one can assume that ELISA is not the preferred method to measure exact concentrations.

3.3.2 Acetylcholine

Achetylcholine (Ach) is an important neurotransmitter to investigate as in AD patients ACh concentrations are strongly decreased. This is the result of the loss of cholinergic neurons. ACh plays an important role in learning and short-term memory, i.e. synaptic plasticity. Hence, the cholinergic system is targeted in current therapy strategies of AD (see 1.4). We measured ACh with a commercial ELISA Kit (Cusabio Biotech Co., Ltd., China). The OD values of the samples were in the middle of the standard curve (between 4 and 5 out of 7 standards measured). In Figure 10 the mean data from the measurement of differently aged groups, each with 3 animals are shown.

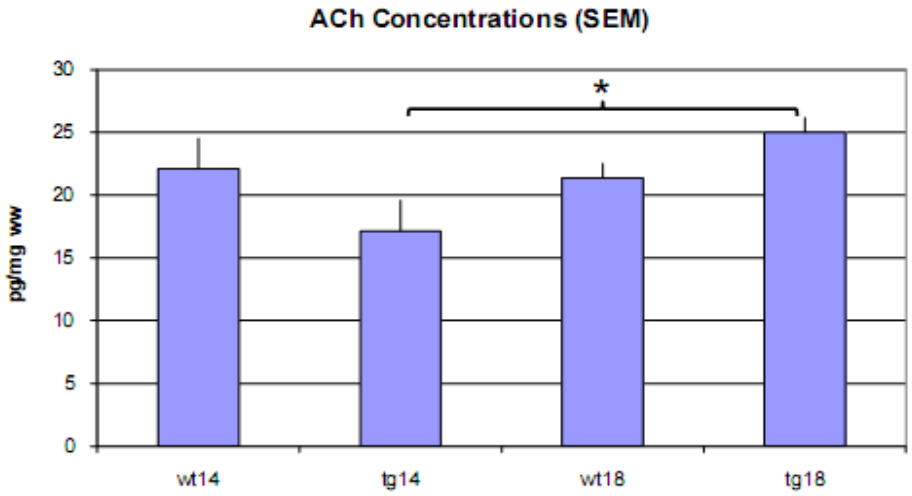

Figure 10: Acetylcholine concentrations in mouse brain homogenates. Measured by ELISA. wt: wildtype, tg: transgenic, 14: 14 months of age, 18: 18 months of age, SEM: standard error of the mean, * - significant (p<0,05),

The only significant difference is detectable between tg animals of the different

ages (for tg14/18: t-test, p=0,045, n=3). This data must be regarded with suspicion as sample number is much too low to suggest a real correlation. To prove that, more samples have to be investigated. No vaccinated transgenic animal samples were analysed. Two research groups published ACh concentrations in mouse brains. They investigated separately different parts of the brain by HPLC-BCD and thus obtained values from 16.4 in the cortex to 27.8nmol/g tissue in the forebrain (without cortex and hippocampus) [53] and 21.4 in the frontal cortex up to 81.8n-mol/g ww in the striatum [54], respectively. After conversion of these values (MW ACh: 146.1g/mol), they reach from 2400pg/mg ww to 12000pg/mg ww. Our values for the whole hemisphere reflects not even a hundredth of the result. Thus, we must assume that also for this kind of measurement the commercial ELISA kit is not suitable.

3.3.3 Dopamine

Dopamine is a neurotransmitter found in subcortical parts of the brain. AD, generally, is designated as cortical dementia, whereas other neurodegenerative diseases like PD and Huntington's disease with dementia symptoms were defined as subcortical forms of dementia [55]. Dopamine levels are decreased since dopaminergic neurons are dying. In PD this influences the extrapyramidal systems and thereby strongly inhibits motor function, leads to depression and slowed cognition (bradyphrenia) [56]. There are reported cases of AD patients with low dopamine levels in the cerebrospinal fluid (CSF) showing the appropriate phenotype [56]. Moreover, dopaminergic neuron loss has been observed in the ventral tegmental area (VTA) [57], a part of the subcortex. Its neurons project into the frontal and limbic areas of the cortex. It is assumed that the changes in the dopaminergic system are secondary to primary arising neuritic plaques in the cortex. This explains why other areas (like the substantia nigra whose neurons project into the basal ganglia where no Aβ deposits are found) are unaffected of dopaminergic neuron loss [57].

We wanted to investigate whether there are any alterations concerning dopamine examining serum and brain homogenates from wildtype and transgenic mice. The sample concentrations never exceeded the OD shown by the blank (dilution buffer provided in the ELISA kit, IBL, Germany)(data not shown). The internal controls al-

ways were in the given range, thus one can conclude that the procedure was carried out properly. In the literature, the levels of dopamine in mouse brains have been reported to be about 970ng/g ww. This has been determined by HPLC-ECD [52]. Our measurements of dopamine levels with the ELISA were not successful and not further conducted.

3.4 Investigation of synaptic alterations

Synapses present connections between neurons and other neurons or non-neuronal cells, respectively. Most neuronal chemical synapses were formed between the axon of the information sending neuron and an dendrite of the neuron which is receiving the information and forwards it to the nucleus. The electrochemical signal arriving at the presynapse is transported via neurotransmitters released from presynaptic vesicles into the synaptic gap. At the postsynapse, neurotransmitters bind to their receptors and thereby transmit the signal to the neighbouring neuron. These mechanisms require intact conditions on both sites of the synaptic gap. Pathologic alterations of pre- and postsynapses (e.g. by induced destabilization and degradation of membrane bound receptors) caused by abnormal protein accumulation, aggregation or decline lead to destruction of the synapse followed by its loss. This in turn is responsible for the eminent decline of memory and cognitive function in neurodegenerative diseases.

3.4.1 Evaluating MAP2 as a dendritic marker via ELISA, Western Blotting and Immunofluorescent Tissue Staining

Dendrites are branches of a neuron. Other than the single axon per nerve cell, one neuron builds up many dendrites. Their function is to submit the electric signal received by another neuron through chemical synapses to the soma of the neuron. The dendritic terminals and dendritic spines (buds along the dendrite) build up many synapses to neighbouring neurons. Thus, they play a central role in signal transmission and in the construction of the neuronal network in the brain.
Microtubuli associated protein 2 (MAP2) is a commonly used marker for dendrites. It stabilizes microtubuli in the dendritic branches, but not in the axon, where this function is fulfilled by Tau protein that is also involved in AD pathology.
The quantification of MAP2 by ELISA (Uscn Life Science Inc., China) was not suc-

cessful. The OD values obtained by analysing the soluble fractions of brain homogenates were never higher than the blank. As blank the dilution buffer provided in the kit was used. From that we must assume that the kit is not suitable for our kind of investigations.

As ELISA was not practicable, we went on to Western Blot analysis of brain homogenates aiming to compare MAP2 concentrations of wildtype and transgenic animals. MAP2 was mainly found in the soluble fraction of the brain homogenates. They were loaded on a gradient gel (NuPAGE) because MAP2 has a very high molecular weight (MW) (about 250kD) and β-actin, used as loading control, a low MW (about 42kD). The 4-12% gradient gel allows separation of all size fractions of interest.

MAP2 shows a triple band at about 250kD whereof the upper two can be related to the two major isoforms of MAP2, MAP2A and -2B (Fig.11). The third one might be another isoform or even more likely translationally modified MAP2 through e.g. phosphorylation.

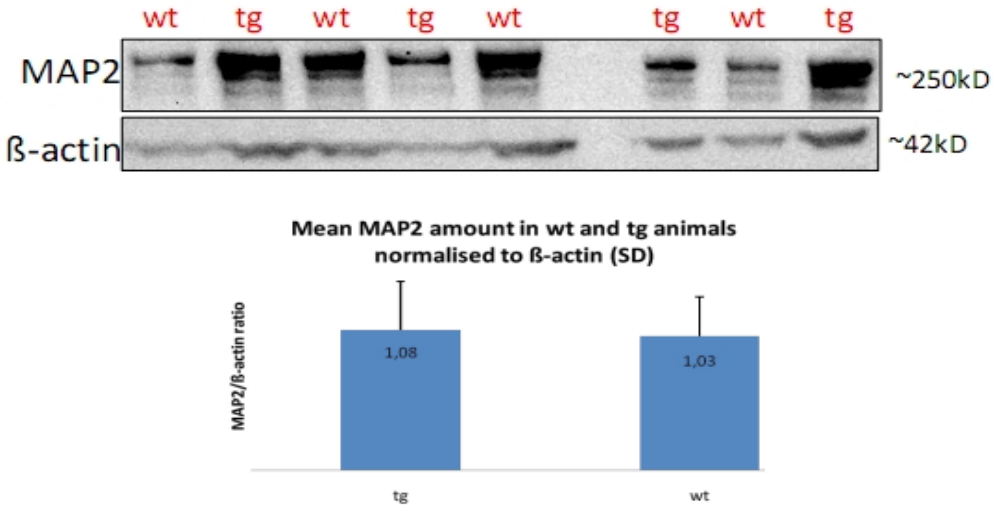

Figure 11: MAP2 Western Blot with soluble fraction of brain homogenates. Protein detection by anti-MAP2 antibody and anti-β-actin as loading control. 14 min exposure time. Corresponding graph showing mean MAP2 values of tg and wt animals normalised to β-actin. SD: standard deviation

Blots were evaluated using the Fiji software program (see chapter 2.3.4.5). There were no differences notable analysing blots on which homogenates of wt and tg single animals were loaded (Fig.11). Nor by calculating blots displaying pooled samples (homogenates of 5 tg or wt animals, respectively were pooled and loaded onto the SDS-PAGE) differences in the MAP2/actin ratio between tg and wt animals

could be detected (data not shown). Therefore we did not go on for further analysis with vaccinated animals.

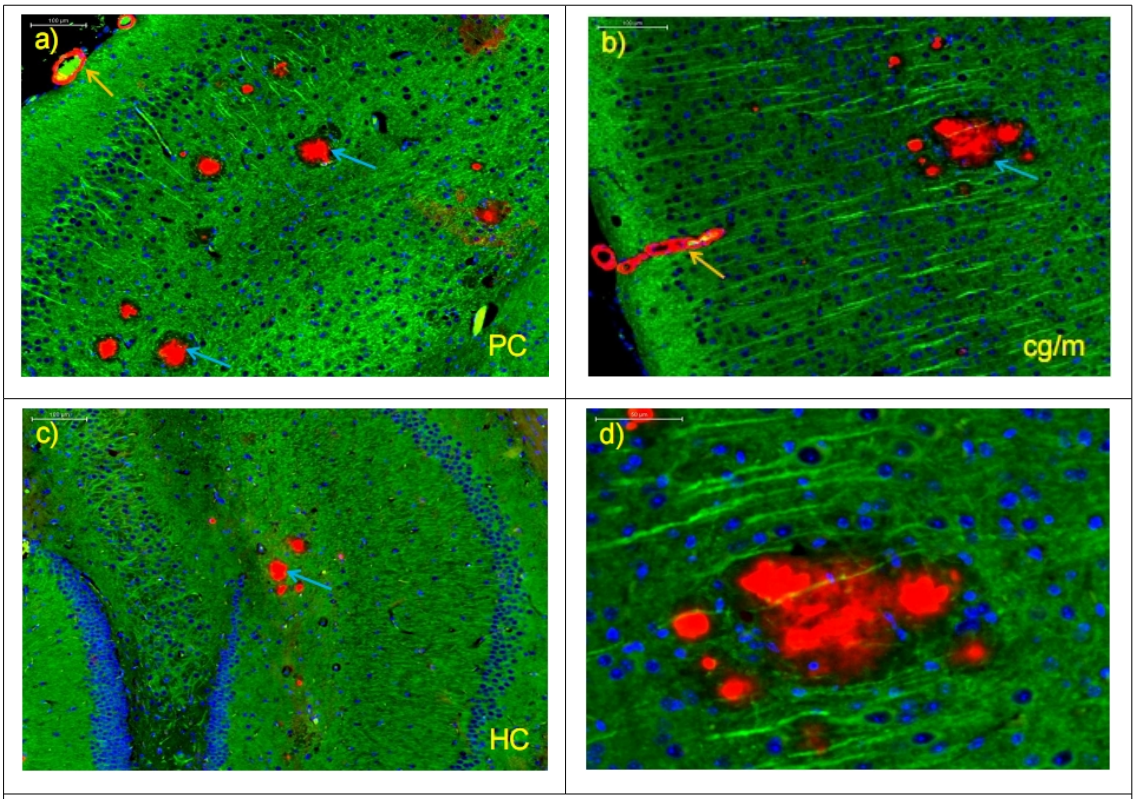

Figure 12: Exemplary chosen amyloid and dendrite double-labelled brain sections, embedded in DAPI containing medium (MV0408, group 1). GFP channel: MAP2->dendrites; Texas Red channel: CR ->amyloid; DAPI channel: DAPI-> cell bodies. a) detail of the parietal cortex; b) detail of cingulate and motor cortex; c) detail of hippocampus; d) magnification of dendrites and amyloid plaques from b). Blue arrows: amyloid deposits; orange arrows: amyloid deposits in blood vessels (CAA)

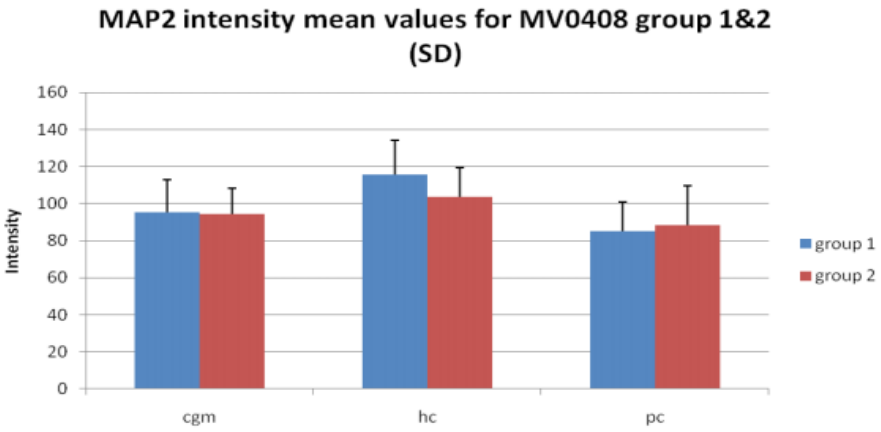

Figure 13: Diagram displaying MAP2 intensities in untreated and AFFITOPE vaccinated animals. Group 1: PBS+Alum; group 2: AD03+Alum; cgm: cingulate and motor cortex, hc: hippocampus, pc: parietal cortex, SD: standard deviation

Next, immunoflourescence staining was done on brain sections. Samples of the experiment MV0408 were stained. As counterstain, Congo Red was used that stains dense cores of congophilic amyloidogenic Aβ aggregates. With the immunohistochemical approach we were aiming to quantify MAP2 positive staining specifically in parts of the brain where AD pathology is observed (Fig.12). These mainly implicate the hippocampus and the cerebral cortex. Fiji software program (version fiji-win32-20100614) was used to measure the intensity of the MAP2 staining in selected areas. We marked three areas of the brain as described for CAA analysis (see chapter 3.4.3.1) (hippocampus, parietal cortex and cingulate and motor cortex) using mirax viewer software (see Fig.20a for details). Briefly, the chosen tissue areas were automatically covered with equally sized, non-overlapping squares by the fiji software program. In each of the squares ten smaller squares were randomly generated by a special makro, so that these squares cover 10% of the selected tissue sample.

In a following step the intensity of the total selected area (e.g. the total marked hippocampus of section one of animal xy) as well as the mean intensity of the small squares were evaluated. For both mean values per group and area were calculated. As there were only slight differences regarding mean total area intensity versus mean small squares intensity, only the latter one was used for result demonstration. The data received are presented in Figure 13. No differences between untreated (group 1) and AFFITOPE vaccinated (group2) transgenic animals were measurable using this approach of image analysis.

3.4.2 Pre- and postsynaptic Markers

For investigation of alterations at the synaptic site, four proteins were chosen. On the one hand three postsynaptic proteins were quantitatively compared by Western Blot. PSD95, Drebrin and ARC/Arg3.1 are located in the dendritic spines where postsynapses were formed. On the other hand, α–synuclein, a small protein located at the presynapse has been investigated.

3.4.2.1 Comparison of PSD95 concentrations in wt and tg animals using Western Blot

Postsynaptic density 95 (PSD95) is a 120 kD protein involved in forming the post-

synapse. We found it in the insoluble fraction of the brain homogenates. For Western Blot analysis insoluble samples had to be dialysed as they cannot be loaded onto gel because of the high detergent concentration (Guanidin-HCl).
PSD95 shows a double band at about 120kD and a light band at about 70kD (Fig.14).

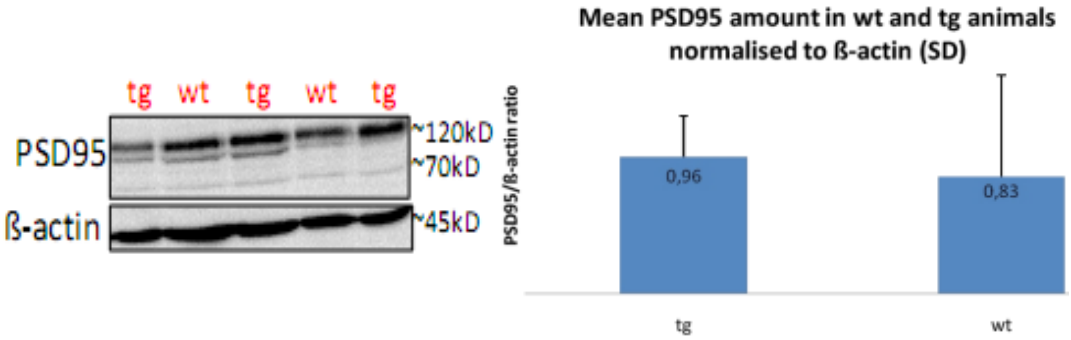

Figure 14: PSD95 Western Blot with dialysed insoluble fraction of brain homogenates. Protein detection by anti-PSD95 antibody and anti-β-actin as loading control. 60 sec exposure time. Corresponding graph showing mean PSD95 values of tg and wt animals normalised to β-actin. SD: standard deviation

After evaluation of the bands by Fiji program, no difference between wt and tg animals has been observed (Fig.14). Also here, the analysis of wt and tg pooled samples did not show a difference in PSD95/actin amount (data not shown). Immunohistochemistry has been performed using this antibody, but only a very weak specific staining could be observed in the hippocampus; not allowing quantitative analysis.

3.4.2.2 Comparison of Drebrin concentrations in wt and tg animals using Western Blot

Drebrin is an actin binding, postsynaptic protein with highest localisation in dendritic spines. Drebrin is best detectable in the insoluble fraction of brain homogenates; i.e. samples had to be dialysed before loading onto gel.
Drebrin migrates at 120kD on the SDS-PAGE (Fig.15). Analysing blots on which single animal samples were loaded, no consistent differences could be detected. Next, pooled wt and tg samples were blotted and analysed, but this again did not show any difference between wt and tg (data not shown). Hence, analysis has not been continued with experiments in vaccinated animals.

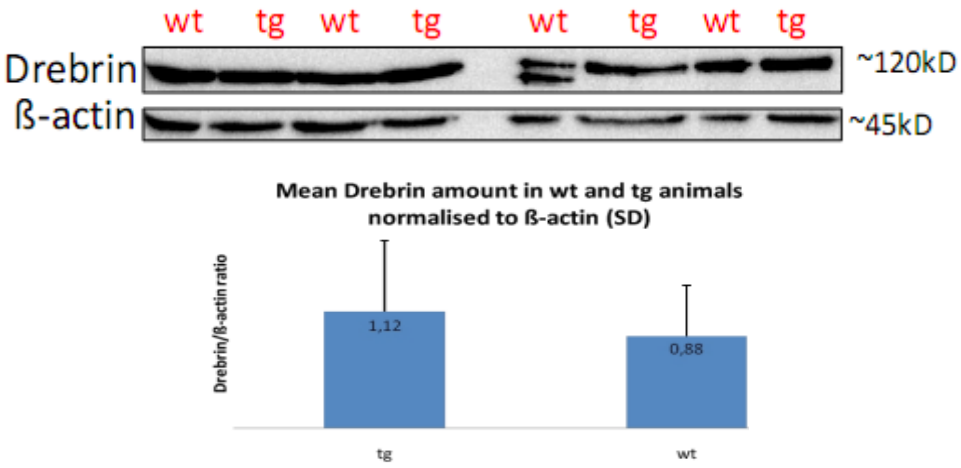

Figure 15: Drebrin Western Blot with dialysed insoluble fraction of mouse brain homogenates. Detection with anti-Drebrin antibody and anti-β-actin antibody. 60sec exposure time. Corresponding graph showing mean Drebrin values of tg and wt animals normalised to β-actin. SD: standard deviation

In addition, immunohistochemical staining with this antibody has been performed. Specificity of the staining was reached using DAB staining, but as there was no possibility for sensible evaluations, no further experiments were carried out.

3.4.2.3 Comparison of ARC/Arg3.1 concentrations in wt and tg animals using Western Blot

ARC/Arg3.1 is also present in dendritic spines. It is an immediate-early gene for memory function and learning processes. The protein is transported to dendritic spines where it is involved in synaptic plasticity. ARC/Arg3.1 is present in the soluble fraction of brain homogenates.

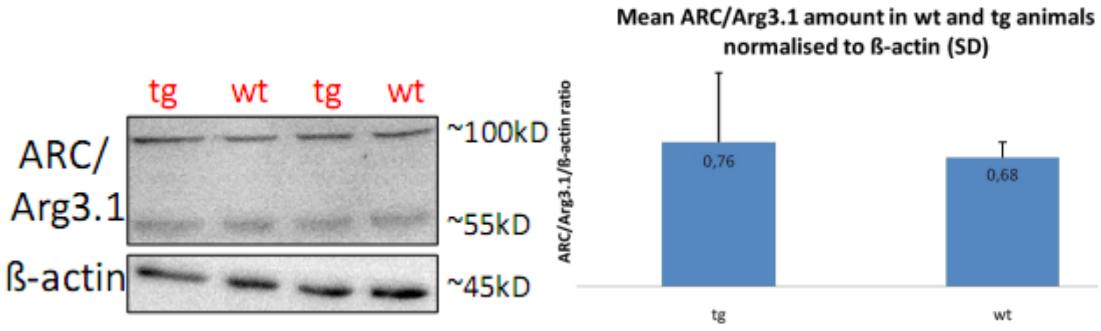

Figure 16: ARC/Arg3.1 Western Blot with soluble fraction of brain homogenates. Protein detection by anti-ARC/Arg3.1 antibody and anti-β-actin as loading control. 5 min exposure time. Corresponding graph showing mean ARC/Arg3.1 values of tg and wt animals normalised to β-actin. SD: standard deviation

ARC/Arg3.1 is reported to migrate between 45 and 55kD on Western Blot (Fig.16) [58], [59]. The upper band might show dimers of the protein even though reducing conditions were chosen for the samples and for the gel. Otherwise it can visualise unspecific binding of the antibody. No changes between wt and tg could be noted (Fig.16), thus the marker was not used for further investigations. This antibody did not give any detectable specific signal in IHC/IF. It is important to keep in mind, that ARC is induced immediately after stimulation with learning events. Therefore, our samples might not be suitable to investigate this protein since the animals were not trained within the last 24h before their death.

3.4.2.4 The presynaptic protein α-synuclein analysed by Western Blotting and Immunoflourescent Staining

α–synuclein is located at the presynapse and therefore can be used as another indicator for the integrity of the synapses. It is found in the soluble fractions in the brain homogenates. First, comparison via Western Blotting was performed.

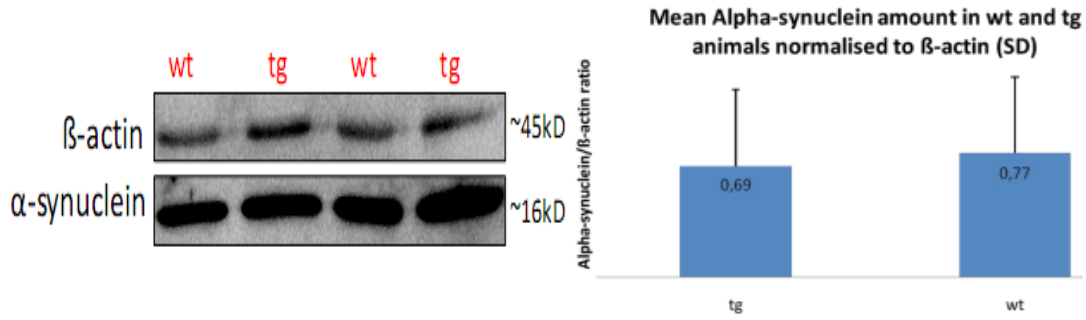

Figure 17: α-synuclein Western Blot with soluble fraction of brain homogenates. Protein detection by anti-α-synuclein antibody and anti-β-actin as loading control. 8 min exposure time. Corresponding graph showing mean α-synuclein values of tg and wt animals normalised to β-actin. SD: standard deviation

By WB no different α-synuclein concentrations could be detected between wt and tg brain homogenates normalised to β-actin (Fig.17). No further comparisons regarding vaccinated animals were carried out.

Next, to investigate single brain areas IF with the same antibody has been performed. Like for MAP2 analysis, brain sections of animals from group 1 and 2 of the MV0408 experiment were stained.

We found specific punctuate staining around amyloid plaques which are mainly loc-

ated in the cerebral cortex and the hippocampus (Fig.18a, b).

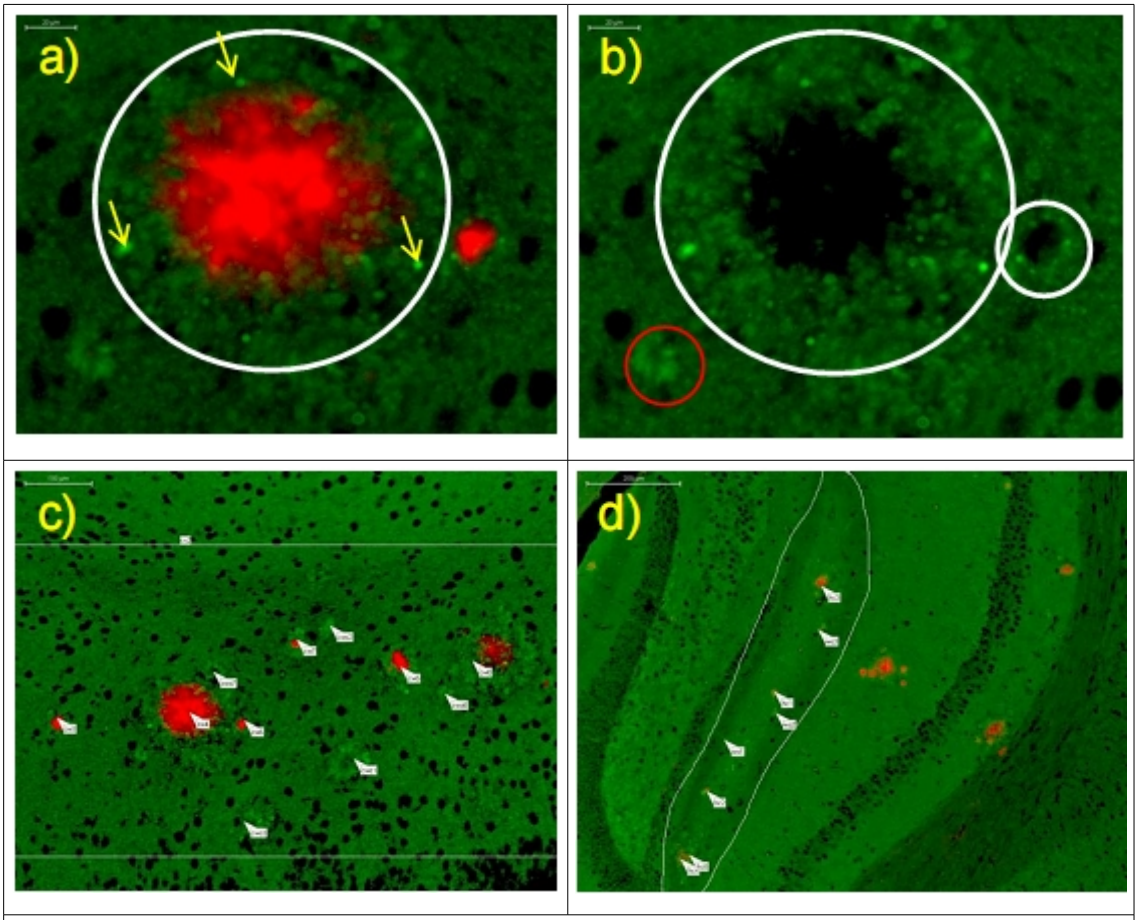

Figure 18: Immunohistochemical staining of α-synuclein on brain sections of Tg2576 mice. GFP channel: α-synuclein; Texas Red channel: CR->amyloid; DAPI channel: DAPI-> cell bodies (gated out). a) amyloidogenic plaque in the cortex surrounded by α-synuclein positive staining (marked with the white circle) made of characteristic α-synuclein occlusions (yellow arrows); example for a CR positive plaque surrounding α-synuclein spot); b) α-synuclein around same plaque-caused lesion in the cortex as in a); the red circle indicates an α-synuclein positive spot without congophilic centre (Texas Red channel gated out); c) example for the selected analysis area in the cortex. α-synuclein positive spots (with and without CR) were marked. d) example for selected analysis area in the hippocampus. α-synuclein positive spots were marked (with and without CR).

This staining is indicating neuritic changes such as degenerative and breaking neurites in the neighbourhood of amyloidogenic plaques. Congo Red staining was performed to counterstain for presence of plaques. This also facilitates the analysis. Additionally, there is also specific α-synuclein staining detectable in the absence of visible or congophilic plaques (some marked spots in Fig.18b,c). These stained areas (“spots”) are characterised by green punctuate abnormalities in areas with high plaque load that mark neuritic alterations. For evaluation, certain areas in the cerebral cortex (parietal cortex) and the hippocampus (exactly the lateral blade of

the molecular layer of the dentate gyrus) were defined. In these two parts of the brain, all α-synuclein-positive spots, with and without CR-positive cores, were counted (Fig.18c, d).

For the demonstration of the data, α-synuclein positive spots surrounding Congo Red stained plaques and only α-synuclein positive stainings are separately shown. The counted number of α-synuclein positive spots were compared between the vaccinated and the non-vaccinated animals in both selected brain areas. The results are depicted in the following diagrams (Fig.19).

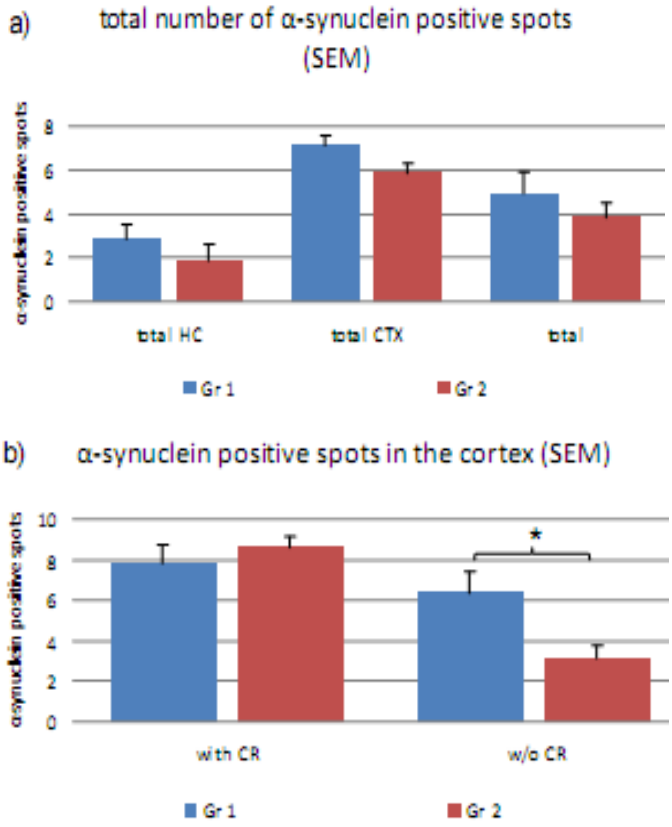

Figure 19: Diagram demonstrating α-synuclein positive spots counted in different areas of the brain. Gr 1: PBS+Alum; Gr 2: AD03+Alum; HC: hippocampus; CTX: cortex; CR: Congo Red; SEM: standard error of the mean, * - significant (p<0,05),

No statistically significant differences between the two groups could be noted in total. A slight decrease in overall α-synuclein positive spots can be assumed (Fig.19a). By examining the spots surrounging congophilic plaques versus α-synuclein staining without visible Aβ deposition, we found statistically significant decrease

of α-synuclein positive spots without CR in the vaccinated animals (Fig.19b; for untreated/vaccinated animals in CTX without CR: t-test, p=0,01, n=14/16). However, no changes were detectable in the amount of α-synuclein spots with CR. The number of counted α-synuclein positive spots in the hc is lower than in the cortex which can be explained by the much smaller size of the investigated hippocampal brain area. In the hippocampus the number of counted spots are very low (from 0 to 4) thus statistical analysis did not make sense. Generally, we can assume the results to indicate a statistically significant (Fig.19b) amelioration of α-synuclein positive neuritic alterations upon amyloid removal.

3.4.3 Alterations coupled to amyloid deposition

Some general pathologic changes that occur in brains of AD patient are cerebral amyloid angiopathy and astrogliosis. The first describes Aβ deposits in blood vessels. The latter is regarding the immune response toward senile plaques.

3.4.3.1 Cerebral Amyloid Angiopathy

Cerebral amyloid angiopathy (CAA) is manifested in vascular deposition of Aβ.
These deposits are congophilic. Hence, the beneficial goal of active vaccination against Aβ would also include an amelioration of CAA in treated animals. An increase of CAA levels could be indication of detrimental alterations in Aβ clearance and could mark a higher risk for damage of brain and brain vasculature following immunotherapy. This analysis in CAA levels is an important confounder of efficacy of active vaccination against Aβ as cerebral amyloid angiopathy can lead to closure of affected blood vessels and be the cause of apoplexia. This could even mark a higher risk for damage in the brain than Aβ plaques do.
We used the Congo Red stained brain sections of MV0408 (CR costaining was done for MAP2 and α-synuclein staining) for CAA analysis (see chapter 3.2). Hence, two consecutive slides of one animal were evaluated to enlarge the number of samples. In three well defined areas of the brain sections (CGM=cingulate and motor cortex, HC=hippocampus and PC=parietal cortex) (Fig.20a)

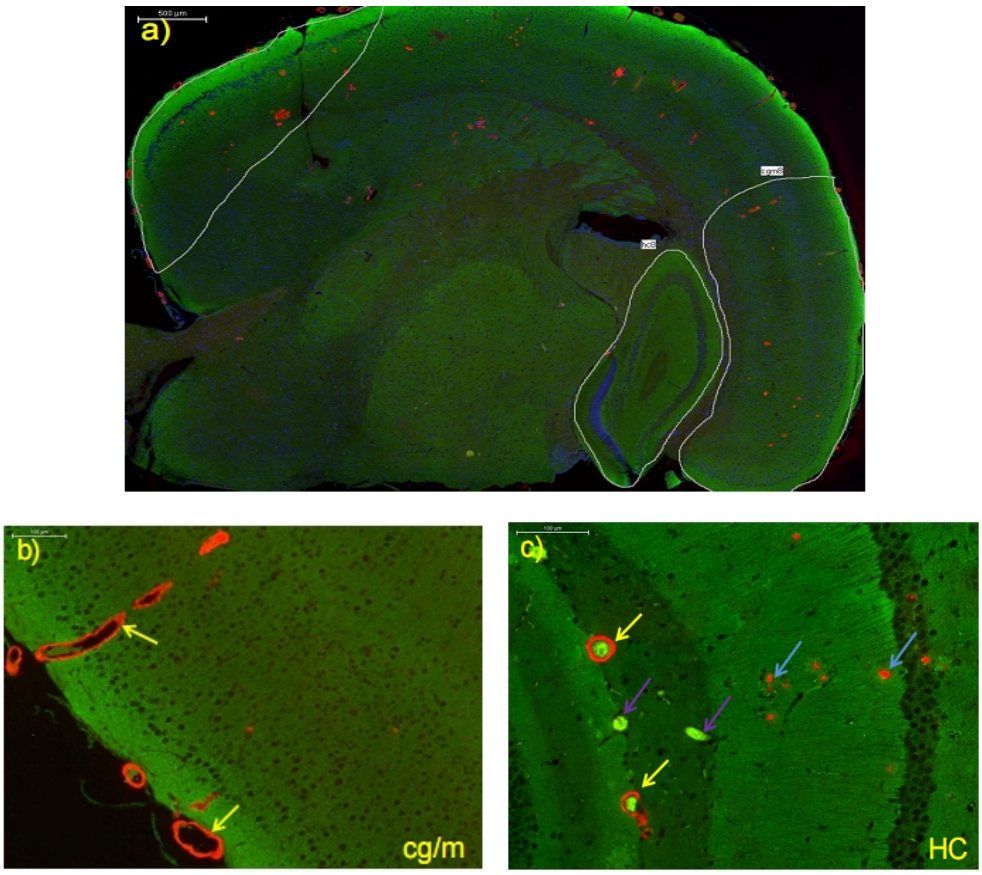

Figure 20: Congo Red staining of amyloid depositions in blood vessels. Texas Red channel: Congo Red; GFP channel: α-synuclein. a) areas of the brain chosen for CAA analysis. b) CAA in the cingulate and motor cortex. c) CAA in the hippocampus. Yellow arrows: CAA. Purple arrows: blood vessels without CAA. Blue arrows: congophilic amyloid plaques.

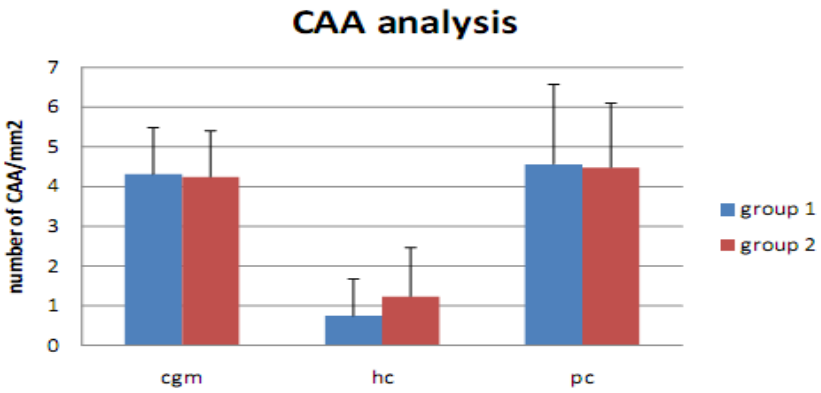

Figure 21: Number of CAA referred to area counted in three parts of the brain. Group 1: PBS+Alum; group 2: AD03+Alum; cgm: cingulate and motor cortex; hc: hippocampus; pc: parietal cortex

Congo Red stained blood vessels were counted. The statistically evaluated data

are shown in the diagram below (Fig.21). We could not find a difference between vaccinated and non-vaccinated transgenic animals. This matches quite well with experiences from other experiments performed in our laboratory. It indicates that CAA pathology is not worsening in immunised mice and demonstrates that active immunization does not exert negative effects on brain functions and the cerebral vasculature.

3.4.3.2 Astrogliosis

To demonstrate the altered immune activity in AD brains, astrocytes were stained on wt, tg and on vaccinated tg mouse brain sections. As expected we could visualise that astrocytes associate with the Aβ deposits in affected brain areas and form so called astrocytic foci.

In Figure 22, parts of the hippocampus and the cortex of wt and differently treated tg animals were shown. Glial fibrillary acidic protein (GFAP) is immunostained and visualised by using Histogreen as substrate (blue-green colour). Neuronal nuclei (NeuN) were visualised by using DAB as substrate (brown colour). Staining reaction of Figures 22c)-d) were stopped earlier than in a) and b), therefore colours are lighter. Additionally, Figures 22c)-d) were counterstained with Congo Red to uncover congophilic amyloid deposits.

It is obvious, that astrocytes aggregate at sites of altered protein accumulation. A tenfold increase of GFAP concentrations has been measured in plaque-containing areas [11]. There, astrocytes are involved in clearance of the neuritic plaques and can be stained by anti-Aβ antibodies. In normal brains they mainly stay in the corpus callosum and are well distributed also in the hc, but never show such clusters as they can be observed in AD brains. No quantitative and statistical evaluation regarding GFAP and NeuN as marker for astrogliosis and neuronal loss, respectively were performed in this analysis.

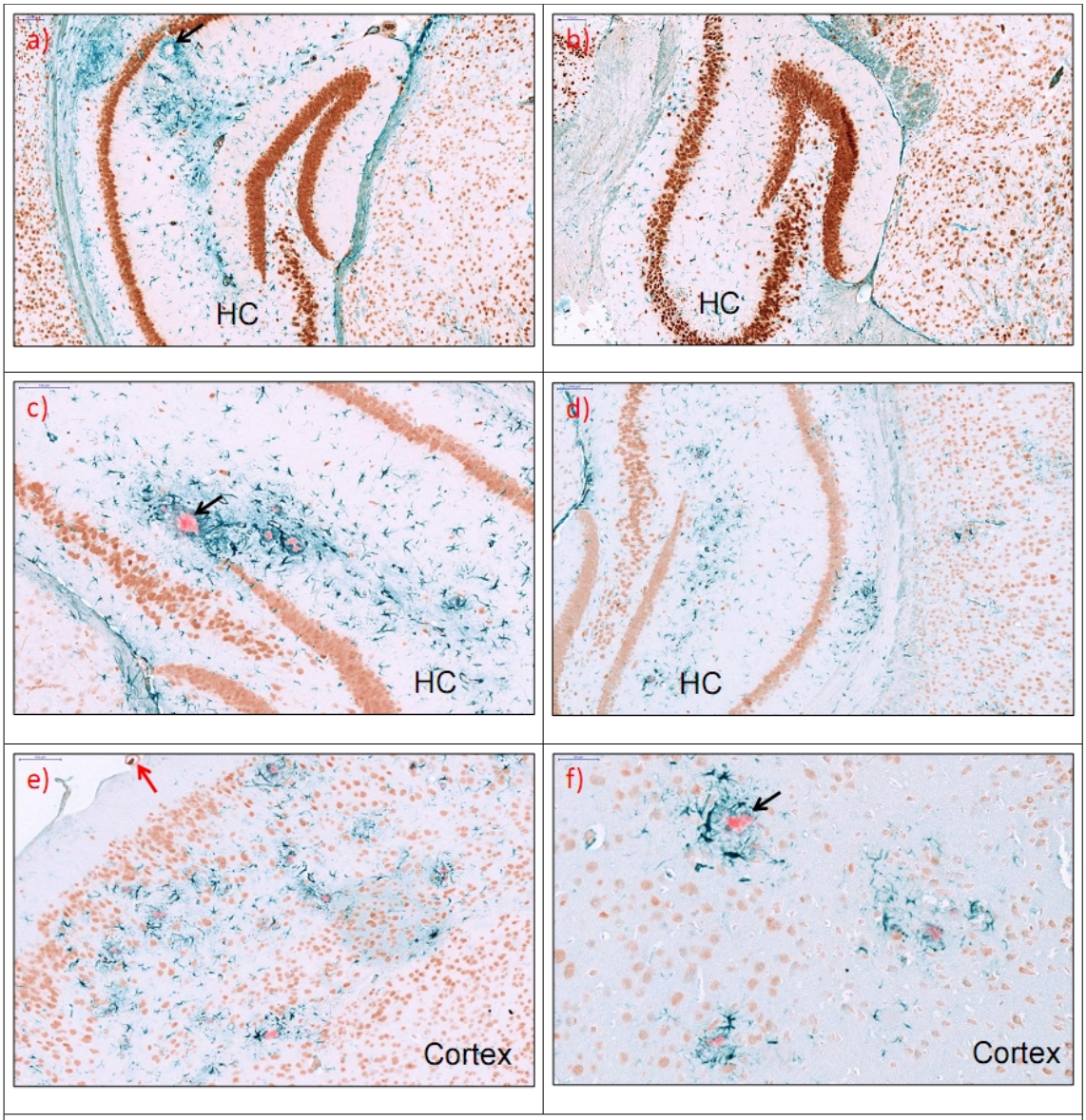

Figure 22: Immunohistochemical staining of neurons and astrocytes (NeuN antibody: brown dye; GFAP antibody: blue-green dye). a) brain section of a <24month old Tg2576 mouse. Astrocytes at the sites of amyloid plaque deposits. b) wt brain sample with equally spreading of astrocytes. c) 18 months old non-vaccinated Tg2576 brain section with characteristic amyloid depositions. d) 18 months old vaccinated tg brain sample. e) cortical area of an untreated animal. d) magnification of cortical astrogliosis. hc: hippocampus; black arrows: not/CR-stained amyloid deposits; red arrow: CR-stained blood vessel

4 Discussion

The aim of the diploma thesis was to investigate whether Tg2576 mice show neuropathologic alterations as observed in AD patients. Moreover, the influence of active immunotherapy against Aβ on these neuropathologic hallmarks should be examined.

Among the investigated factors was the neurotrophic APP metabolite sAPPα. With the commercial ELISA kit we did not measure any significant changes in the concentrations of human and murine sAPPα in the soluble fraction of brain homogenates of differently vaccinated and untreated animals. It has been shown that sAPPα has a slower turnover in Tg2576 animals than in wildtype mice [60]. Indeed it has been demonstrated that an amyloid plaques containing brain needs more neurotrophic support [61]. That means that even higher levels of sAPPα were to be measured in transgenic mice than in wildtype mice. These findings are in line with the results we obtained by measuring wt and tg animals (see Fig.7). Tapia-Aranicibia et al. assume that sAPPα counteracts the neurotoxic influence of Aβ plaques in AD brains. In APP transgenic mouse model, undoubtedly human sAPPα as well as human Aβ are produced both in high quantities as the APP gene possesses a strong promoter (see chapter 1.5) and the mutation enhances γ–secretase activity [62].
Finally we can conclude that sAPPα levels are not negatively affected by the vaccination. Above all this is of interest for the murine sAPPα levels. It would be devastating when induced antibodies would crossreact with the neurotrophic factor. This could even worsen memory and cognitive functions instead of ameliorating them as protection and rescue mechanisms implying sAPPα get lost.

Next, our investigations focused on different neurotransmitters. Again, we used commercial ELISA kits. We did not obtain any differences between soluble fractions of brain homogenates of wt and tg animals concerning neurotransmitter levels. There are several explanations for that. On the one hand we analysed whole hemibrains. This kind of approach does not allow the measurement of little changes

in small areas of the brain. As the cholinergic system mainly influences the hippocampus and cerebral cortex, it might be possible to measure different amounts of ACh in tg and wt animals observing only these regions. Likewise, serotonin is used by only 0.1-1% of all synapses. It is produced in the Raphe nucleus located in the brain stem and is active in the cortex and cerebellum. By separately analysing these parts of the brain, chances of detecting differences could be augmented. The same is true for dopamine which is used by about 15% of all nerve cells in the striatum and is very rare in the rest of the brain. On the other hand one might have to use another method unlike ELISA. As mentioned in chapter 3.3, researchers were able to measure neurotransmitter levels in different brain areas by using HPLC-ED in separated areas of mouse brains [52-54].

The next step in the project was the investigation of pre- and postsynaptic alterations in APP transgenic animals. Therefore, we did Western Blot analysis of brain lysates of wt and tg animals using antibodies specific for different pre- and postsynaptic markers as well as one dendritic marker.
ARC/Arg3.1 (activity-regulated cytoskeleton-associated protein) is an immediate-early gene. Its mRNA is induced following stimulation of long term potentiation (LTP) and transported to dendrites, where it is meant to be translated [63]. ARC/Arg3.1 plays a essential role in the process of learning and memory as well as in synapse plasticity. Complete KO mice (ARC/Arg3.1$^{-/-}$) showed a much lower performance in long-term memory tests (MWM, context dependent fear conditioning, taste aversion memory) than wildtype animals did indicating an impaired function in memory and learning. Synapse plasticity is the ability of a synapse between two neurons to change its strength. It is build up via LTP and LTD (long term depression). ARC/Arg3.1 loss of function mutants show an increase in LTP and a decrease in LTD. The discoverers assume that this fact is linked to the decreased endocytosis of the AMPA receptor (a glutamate receptor) that is ARC/Arg3.1 mediated [64]. Thirty minutes after memory training, ARC/Arg3.1 is upregulated [65], [66]. This very fast response might be an explanation why we could not detect any difference between tg and wt animals. The animals were not trained before they were sacrificed. In AD patients, initial increase followed by a decrease of ARC/Arg3.1 has been observed. Short exposure to Aβ oligomers enhance ARC/Arg3.1 expression;

in contrast long exposure reduce ARC/Arg3.1 basal levels as well as its induction in learning situations [67].

Drebrin (developmentally regulated brain protein) is an actin binding protein [68]. Its molecular weight is about 70kD, but in electrophoresis it also shows a particular 120kD band [69]. The isoform Drebrin A is neuron-specific and mainly located in dendrites, particularly in dendritic spines [70], whose biochemical properties, size and form are crucial for synaptic transmission. Moreover it is involved in the morphogenesis of dendritic spines. Drebrin A is required for the clustering of PSD95 as well as for synapse plasticity [71]. Low concentrations of Drebrin A have been associated with trisomy 21 and AD [72]. A decline of Drebrin has been shown in Tg2576 [73], [74] as well but could not be reproduced by our analysis.

PSD95 (post synaptic density 95) is a member of the membrane-associated guanylate kinase (MAGUK) family. It contains a PDZ domain, which consists of 80-90 aa allowing to bind a peptide sequence at the C-Terminus of other specific proteins. PSD95 is involved in anchoring synaptic proteins as well as clustering and organisation of receptors such as NMDARs at the synapses [75], [76]. Moreover, it can drive synaptic maturation at post- but also at presynaptic terminals. Its overexpression showed an increase of the number and the size of dendritic spines [77].

The presynaptic protein α-synuclein is best known from PD where it forms aggregates, so called Lewy bodies, the main pathologic hallmark of this disease. It is also found in DLB, a form of dementia with Lewy bodies (intraneural aggregation of α-synuclein near the nucleus). There, it has been shown that dendritic spine retraction occur rather than complete synapse loss. This is particularly true if there are α-synuclein aggregates at the presynaptic sites. The researchers found reduction of the pre- and postsynaptic markers (synaptophysin and PSD95) in DLB patients compared to non-demented persons and complete loss of Drebrin [78]. The same phenomenon could be noted in neostriatal medium spiny neurons in PD [79]. Concluding, it is important to underline the fact that size and number of dendritic spines are associated with memory. Inducing LTP leads to the formations of new dendritic spines [80].

We did not detect any differences between tg and wt animals concerning these factors. As mentioned above in the discussion of the ELISA results, the same is true for the WB results. When there are small alterations in tg animals compared to

wt animals in dedicated areas of the brain, analysis of the full hemibrain might preclude to detect these subtle differences. Also here it applies that only the regions of interest should be analysed. In all cases this would implicate the hippocampus and the cerebral cortex because there both, the amyloid plaque load and neuron density is the highest. This can be done by either preparation of the single brain areas followed by biochemical analysis or by region specific immunohistochemical stainings on brain sections.

The latter has been performed in the case of α-synuclein and MAP2 antibodies. Immunohistochemistry of MAP2 gave good insight to the structure and arrangement of dendrites in different brain layers. Even by eye alterations near neuritic plaques were easily detectable. Nevertheless, measurements of MAP2 intensities in different brain areas did not show amelioration in vaccinated versus untreated transgenic animals. We suppose the magnification and resolution of the microscope as well as the thickness of the tissue samples (7µm) to be the most problematic factors in the type of analysis we performed. There are published data about dendritic spine loss in the mouse model we were using. Lanz et al. found dendritic spine loss in CA1 hippocampal neurons and referred that on ageing and APP overexpression [81]. Besides, Spires-Jones et al. established the theory stating plaques to be space-occupying lesions in whose immediate neighbourhood loss of dendrites occurs. However, amyloid plaques are thought to spread even farer [82]. In these farther areas, soluble Aβ is predicted to be responsible for PSD95 reduction at the site of dendritic spines and following AMPAR internalisation [83]. This leads to the breakdown of spines [84]. Dystrophic neurites have been observed in the direct neighbourhood of plaques. They only arise at the second day of plaque formation or even later indicating that the damage caused to the neurons are caused by Aβ plaques [85]. Concluding we can suggest that either the methods we used and the approach of analysis that has been chosen are not the best suitable for such kind of investigations.

The immunoflourescence staining of α-synuclein was successful as well and we were able to count the positive stained spots around congophilic amyloidogenic deposits and smaller spots without visible plaque associated. As the amyloid plaque

load in the therapeutic experiment is 36% decreased in the vaccinated group in comparison to the PBS control group (see chapter 3.2, Fig.8a) we would also expect less neuritic alterations in these animals. In total, we found an insignificant decline in total α-synuclein-positive stainings. Statistically significant results were obtained in the cortex when counting α-synuclein positive spots devoid of visible congophilic deposits. This leads to the conclusion that active immunization against Aβ in mice leads to clearance of soluble Aβ and to the removal of dense core congophilic Aβ plaques. By the elimination of these small rather soluble Aβ depositions also neuritic alterations indicated by α-synuclein positive punctuate abnormalities seem to be diminished.

A certain part of α-synuclein is reported to take part in amyloid plaques as the so called non amyloid component (NAC) [86-88]. This is the domain in the α-synuclein protein which is responsible for its high prevalence to aggregate and is involved in Lewy body formation in PD. One must notice that the α-synuclein staining as we found it, is not identical with NAC because other than NAC we found staining around but not in the plaques. Yang et al. also observed the punctuate accumulation of α-synuclein along the perimeter of the plaques in Tg2576 animals [88]. They suggest a defect in the proteasome system might be the cause of α-synuclein accumulation that is also reported to be linked to PD. α-synuclein usually is degraded via ubiquitination and following proteasomal degradation. Similar observations to ours were made with synaptophysin [89] which is also a presynaptic protein. Dong et al. neither found changes in tg and wt animal in overall synaptophysin-positive bouton (presynaptic bud) density using quantitative light microscopy. However, with electron microscopy they were able to reveal a significant overall decline in synaptic density in tg animals compared to non-transgenic littermates. The analysed parts of the brain comprise the outer molecular layer of the dentate gyrus and the entorhinal cortex (comparable to the areas we investigated). Additionally, they state a correlation between the proximity to amyloid plaques and decrease of synaptic density. Finally they assume that the stained presynaptic spots arise after rearrangement of presynaptic proteins provoked by the degeneration of postsynapses that are depicted in other studies [90].

5 Conclusion

In our research of Tg2576 we found slight impairments on the synaptic networks compared to a wildtype laboratory mouse strain. These changes were visualised on the one hand by MAP2 staining in the immediate neighbourhood of amyloid deposits. MAP2 reflects the amount of dendrites and their branches, which are highly involved in synapse formation. In transgenic animals the networks of dendrites are impaired in certain regions of the brain such as the cortex and the hippocampus. This results from amyloid deposits spread in these areas. On the other hand accumulation of α-synuclein around neuritic plaques allows assumption of worse synaptic function. Soluble α-synuclein usually is present in nearly all areas of the brain and is involved in synapse rearrangement at presynaptic sites. Statistically significant differences between vaccinated and non-vaccinated animals could not be shown with the methods we used. Hence, for more insight in whether in our mouse model, synapse density and plasticity is improved after vaccination, methods with higher resolution have to be used, like confocal microscopy.

The investigated postsynaptic proteins PSD95, Drebrin and ARC/Arg3.1 were not further analysed as no different concentrations in wildtype and transgenic animals were detectable by Western Blotting. Again, one possibility to detect marginal changes in some areas of the brain more sensitive methods have to be used. These would include biochemical analysis of only distinct parts of the brain instead of whole hemibrains. Otherwise immunohistochemical protocols can be established that allow quantitative analysis.

This also holds true for the investigation of neurotransmitters. Every transmitter is responsible for special neuronal cell types. These are not regularly spread in the whole brain, but with high accumulation in certain areas. Thus, an effect of the transgene might be detectable by analysing single brain areas separately. By analysing hemibrains we were not able to show any differences. Another explanation for that would be that neuronal loss, observed in AD patients [91-93], has not be noted in Tg2576 animals [11]. Death of e.g. cholinergic neurons leads to a decrease of acetylcholine in the affected brain area. Another reason for the unsatisfying results could be the insufficiency of the commercial kits used for the analysis.

Hence, one can say, that for further studying positive impacts of active immunization against Aβ apart from plaque clearance and improvement of cognitive functions (Mandler et al., manuscript in preparation), one possibility would be to use a different animal model, which shows a stronger phenotype regarding pathologic hallmarks of AD such as neuronal loss. There are more aggressive mouse models available and showing impaired neurotransmission such as the APP23 mouse [94]. Mouse models known to show neuronal loss and synaptic dysfunction mostly have different mutations in the human APP transgene that is under the control of a neuron specific promoter and leads to overexpression. In addition, they carry other transgenes with mutations in the PS1 gene, a crucial part of the γ–secretase protein complex responsible for Aβ production [95].
Another possibility to get insight into neuropathologic alterations would be to look carefully on the patients participating in the clinical trials. Studying their brains post mortem with regard to their symptomatic amelioration in context with synapse and neuron loss could be most illuminative.

In conclusion, we can assume amelioration in vaccinated mice regarding all markers which are in the immediate neighbourhood of neuritic plaques, such as astrocytosis (Mandler et al., manuscript in preparation), density of dendrites, neuritic and presynaptic alterations as well as cognitive function. This gives hope for beneficial properties of the vaccine on AD associated alterations also in humans.

References

[1] Terry, RD, Katzman, R., Bick, KL, and Sisodia, SS, *Alzheimer Disease*, 2. ed. Lippincott Williams & Wilkins, 1999.

[2] H. Förstl and A. Kurz, “Clinical features of Alzheimer’s disease,” *European Archives of Psychiatry and Clinical Neuroscience*, vol. 249, no. 6, pp. 288–290, 1999.

[3] Alzheimer, A., “Über eine eigenartige Erkrankung der Hirnrinde,” *Allg. Zeitschrift für Psychiatrie und psychisch-gerichtliche Medizin*, no. 64, pp. 146-148, 1907.

[4] H. L. Weiner and D. Frenkel, “Immunology and immunotherapy of Alzheimer's disease,” *Nature Reviews Immunology*, vol. 6, no. 5, pp. 404–416, 2006.

[5] Mark P. Mattson, “Pathways towards and away from Alzheimer's disease,” *Nature*, no. 430, pp. 631-639, 2004.

[6] F. M. LaFerla, “Calcium dyshomeostasis and intracellular signalling in Alzheimer's disease,” *Nature Reviews. Neuroscience*, vol. 3, no. 11, pp. 862-872, Nov. 2002.

[7] Hardy, “Amyloid, the presenilins and alzheimer's disease,” *Trends in Neuroscience*, no. 20, pp. 154-159, 1997.

[8] Citron, M., “Alzheimer's disease: strategies for disease modification,” *Nature Reviews Drug Discovery*, no. 9, pp. 387-398, 2010.

[9] K. Blennow, M. J. de Leon, and H. Zetterberg, “Alzheimer's Disease,” *Lancet*, vol. 368, pp. 387–403, 2006.

[10] D. J. Selkoe, “Alzheimer's disease: genes, proteins, and therapy,” *Physiological reviews*, vol. 81, no. 2, p. 741, 2001.

[11] C. Duyckaerts, M. Potier, and B. Delatour, “Alzheimer disease models and human neuropathology: similarities and differences,” *Acta Neuropathologica*, vol. 115, no. 1, pp. 5-38, 2007.

[12] G. Thinakaran and E. H. Koo, “Amyloid Precursor Protein Trafficking, Processing, and Function,” *Journal of Biological Chemistry*, vol. 283, no. 44, pp. 29615-29619, 2008.

[13] Suh, YH and F. Checler, F., “Amyloid Precursor Protein, Presenilins, and α-Synuclein: Molecular Pathogenesis and Pharmacological Applications in Alzheimer's Disease,” *Pharmacological Reviews*, no. 54, pp. 469-525, 2002.

[14] D. E. Schmechel et al., “Increased amyloid beta-peptide deposition in cerebral cortex as a consequence of apolipoprotein E genotype in late-onset Alzheimer disease,” *Proceedings of the National Academy of Sciences of the United States*

of America, vol. 90, no. 20, p. 9649, 1993.

[15] Krämer, G. and Förstl, H., *Alzheimer & andere Demenzen: Antworten auf die häufigsten Fragen*, 5. ed. Trias, 2008.

[16] R. Tanzi and L. Bertram, “Twenty Years of the Alzheimer?s Disease Amyloid Hypothesis: A Genetic Perspective,” *Cell*, vol. 120, no. 4, pp. 545-555, 2005.

[17] W. J. Brecht et al., “Neuron-SpecificApolipoproteinE4ProteolysisIsAssociated withIncreasedTauPhosphorylationinBrainsof TransgenicMice,” 2004.

[18] E. M. Mandelkow and E. Mandelkow, “Tau in Alzheimer's disease,” *Trends in cell biology*, vol. 8, no. 11, pp. 425–427, 1998.

[19] Henning-Jensen, P., Hager, H., Nielsen, MS, Hojrup, P., Gliemann, J., and Jakes, R., “α-Synuclein Binds to Tau and Stimulates the Protein Kinase A-catalyzed Tau Phosphorylation of Serine Residues 262 and 356,” *The Journal of Biological Chemistry*, no. 274, pp. 25481-25489, 1999.

[20] D. W. Dickson, “Neuropathology of non-Alzheimer degenerative disorders,” *International journal of clinical and experimental pathology*, vol. 3, no. 1, p. 1, 2010.

[21] H. Zheng and E. H. Koo, “The amyloid precursor protein: beyond amyloid,” *Molecular neurodegeneration*, vol. 1, p. 5, 2006.

[22] T. Matsui et al., “Expression of APP pathway mRNAs and proteins in Alzheimer's disease,” *Brain research*, vol. 1161, pp. 116–123, 2007.

[23] H. Lassmann, P. Fischer, and K. Jellinger, RF, “Synaptic Pathology of Alzheimer's,” *Alzheimer's disease: amyloid precursor proteins, signal transduction, and neuronal transplantation*, p. 59, 1993.

[24] Van Dam, D. and De Deyn, P., “Drug discovery in dementia: the role of rodent models,” *Nature Reviews Drug Discovery*, vol. 5, pp. 956-970, 2008.

[25] Golde, TE, Eckman, CB, and Younkin, SG, “Biochemical detection of Aβ isoforms: implications for pathogenesis, diagnosis, and treatment of Alzheimer’s disease,” *Biochimica et Biophysica Acta (BBA)-Molecular Basis of Disease*, no. 1502, pp. 172-187, 2000.

[26] M. P. Mattson, “Cellular actions of beta-amyloid precursor protein and its soluble and fibrillogenic derivatives,” *Physiological reviews*, vol. 77, no. 4, p. 1081, 1997.

[27] Lansbury Jr., P. and Griffin, R., “Structural model for the bold beta-amyloid fibril based on interstrand alignment of an antiparallel-sheet comprising a C-terminal peptide,” *Nature Structural Biology*, no. 2, pp. 990 - 998, 1995.

[28] N. Gakhar-Koppole et al., “Activity requires soluble amyloid precursor protein al-

pha to promote neurite outgrowth in neural stem cell-derived neurons via activation of the MAPK pathway," *The European Journal of Neuroscience*, vol. 28, no. 5, pp. 871-882, Sep. 2008.

[29] P. Turner,, K. O'Connor, W. Tate, and W. Abraham, "Roles of amyloid precursor protein and its fragments regulating neural activity, plasticity and memory," *Progress in Neurobiology*, no. 70, pp. 1-32, 2003.

[30] M. Racchi and S. Govoni, "The pharmacology of amyloid precursor protein processing," *Experimental gerontology*, vol. 38, no. 1, pp. 145–157, 2003.

[31] T. Kawarabayashi, L. H. Younkin, T. C. Saido, M. Shoji, K. H. Ashe, and S. G. Younkin, "Age-dependent changes in brain, CSF, and plasma amyloid beta protein in the Tg2576 transgenic mouse model of Alzheimer's disease," *Journal of Neuroscience*, vol. 21, no. 2, p. 372, 2001.

[32] Priller, C., "Funktion des Amyloid Precursor Proteins und dessen Spaltprodukten bei der synaptischen Übertragung," LMU, 2006.

[33] Oda, "Clusterin (apoJ) Alters the Aggregation of Amyloid β-Peptide (Aβ1-42) and Forms Slowly Sedimenting Aβ Complexes That Cause Oxidative Stress," *Experimental Neurology*, no. 136, pp. 22-31, 1995.

[34] P. D. Coleman and P. J. Yao, "Synaptic slaughter in Alzheimer's disease," *Neurobiology of aging*, vol. 24, no. 8, pp. 1023–1027, 2003.

[35] Callahan, LM, "Quantitative decrease in synaptophysin message expression and increase in cathepsin D message expression in Alzheimer disease neurons containing neurofibrillary tangles.," *Journal of Neuropathology and experimental neurology*, no. 58, pp. 275-87, 1999.

[36] T. Wisniewski and A. Boutajangout, "Vaccination as a Therapeutic Approach to Alzheimer's Disease," *Mount Sinai Journal of Medicine: A Journal of Translational and Personalized Medicine*, vol. 77, no. 1, pp. 17–31, 2010.

[37] H. Dong, C. A. Csernansky, M. V. Martin, A. Bertchume, D. Vallera, and J. G. Csernansky, "Acetylcholinesterase inhibitors ameliorate behavioral deficits in the Tg2576 mouse model of Alzheimer's disease," *Psychopharmacology*, vol. 181, no. 1, pp. 145–152, 2005.

[38] M. Langlois, F. Van Leuven, S. Sicsic, and A. M. Gardier, "5-HT4 receptor agonists increase sAPPa levels in the cortex and hippocampus of male C57BL/6j mice," *British Journal of Pharmacology*, vol. 150, pp. 883–892, 2007.

[39] P. Raina et al., "Effectiveness of cholinesterase inhibitors and memantine for treat-

ing dementia: evidence review for a clinical practice guideline," *Annals of internal medicine*, vol. 148, no. 5, p. 379, 2008.

[40] Abbas, AK, Lichtman, AH, and Pillai, S., *Cellular and Molecular Immunology*. Elsevier, 2007.

[41] M. Lee et al., "A beta 42 immunization in Alzheimer's disease generates A beta N-terminal antibodies," *Annals of neurology*, vol. 58, no. 3, pp. 430–435, 2005.

[42] A. Schneeberger, M. Mandler, O. Otava, W. Zauner, F. Mattner, and W. Schmidt, "Development of AFFITOPE vaccines for Alzheimer's disease (AD)—From concept to clinical testing," *The Journal of Nutrition, Health and Aging*, vol. 13, no. 3, pp. 264–267, 2009.

[43] Schneeberger, A., Mandler, M., F. Mattner, and W. Schmidt, "AFFITOME® technology in neurodegenerative diseases: The doubling advantage," *Human Vaccines*, vol. 6, no. 11, pp. 1-5, 2010.

[44] D. Schenk, D., "Amyloid-ß immunotherapy for Alzheimer's Disease: the end of the beginning," *Nature Reviews Neuroscience*, no. 3, pp. 824-828, 2002.

[45] D. Moechars et al., "Early phenotypic changes in transgenic mice that overexpress different mutants of amyloid precursor protein in brain," *Journal of Biological Chemistry*, vol. 274, no. 10, p. 6483, 1999.

[46] Hsiao K et al., "Correlative memory deficits, Abeta elevation, and amyloid plaques in transgenic mice," *Science*, no. 274, pp. 99-102, 1996.

[47] P. F. Chapman et al., "Impaired synaptic plasticity and learning in aged amyloid precursor protein transgenic mice," *Nature neuroscience*, vol. 2, no. 3, pp. 271–276, 1999.

[48] S. Gravina, "Amyloid β Protein (Aβ) in Alzheimeri's Disease Brain Biochemical and immunocytochemical analysis with antibodies specific for forms ending at Aβ40 or Aβ42(43)," *The Journal of Biological Chemistry*, no. 270, pp. 7013-7016, 1995.

[49] M. A. Westerman et al., "The relationship between Abeta and memory in the Tg2576 mouse model of Alzheimer's disease," *Journal of Neuroscience*, vol. 22, no. 5, p. 1858, 2002.

[50] D. M. Mann and P. O. Yates, "Serotonin nerve cells in Alzheimer's disease.," *Journal of Neurology, Neurosurgery & Psychiatry*, vol. 46, no. 1, p. 96, 1983.

[51] Francis, PT, "The Interplay of Neurotransmitters in Alzheimer's Disease," *CNS Spectrums*, vol. 11, no. 10, pp. 6-9, 2005.

[52] S. Sasa and C. L. Blank, “Determination of serotonin and dopamine in mouse brain tissue by high performance liquid chromatography with electrochemical detection,” *Analytical Chemistry*, vol. 49, no. 3, pp. 354–359, 1977.

[53] S. Y. Chung et al., “Administration of phosphatidylcholine increases brain acetylcholine concentration and improves memory in mice with dementia,” *Journal of Nutrition*, vol. 125, no. 6, p. 1484, 1995.

[54] M. Iwai, K. Suzuki, O. Moriai, A. Kato, S. Sato, and S. Murai, “Decreased brain concentrations of choline and acetylcholine in mice with thioacetamide-induced acute liver failure,” *International Hepatology Communications*, vol. 3, no. 4, pp. 222–226, 1995.

[55] M. A. Turner, N. F. Moran, and M. D. Kopelman, “Subcortical dementia,” *The British Journal of Psychiatry*, vol. 180, no. 2, p. 148, 2002.

[56] N. Wolfe et al., “Neuropsychological profile linked to low dopamine: in Alzheimer's disease, major depression, and Parkinson's disease.,” *British Medical Journal*, vol. 53, no. 10, p. 915, 1990.

[57] D. M. Mann, P. O. Yates, and B. Marcyniuk, “Dopaminergic neurotransmitter systems in Alzheimer's disease and in Down's syndrome at middle age.,” *British Medical Journal*, vol. 50, no. 3, p. 341, 1987.

[58] “http://www.acris-antibodies.com/target/arc-arg3-1-antibody.htm.”

[59] Johns Hopkins University, “Arc and synapic platicity,” *BioWave*, vol. 16, no. 10, 2008.

[60] J. Morales-Corraliza et al., “In Vivo Turnover of Tau and APP Metabolites in the Brains of Wild-Type and Tg2576 Mice: Greater Stability of sAPP in the β-Amyloid Depositing Mice,” *PLoS ONE*, vol. 4, no. 9, p. e7134, 2009.

[61] L. Tapia-Aranicibia, E. Aliaga, M. Silhol, and S. Arancibia, “New insights into brain BDNF function in normal aging and Alzheimer disease,” *Brain Research Reviews*, no. 59, pp. 201–220, 2008.

[62] Citron, M., Oltersdorf, T., and Haass, C., “Mutation of the beta-amyloid precursor protein in familial Alzheimer's disease increases beta-protein production,” *Nature*, no. 360, pp. 672-674, 1992.

[63] W. Link et al., “Somatodendritic expression of an immediate early gene is regulated by synaptic activity,” *Proceedings of the National Academy of Sciences of the United States of America*, vol. 92, no. 12, p. 5734, 1995.

[64] N. Plath et al., “Arc/Arg3. 1 is essential for the consolidation of synaptic plasticity

and memories," *Neuron*, vol. 52, no. 3, pp. 437–444, 2006.

[65] C. R. Bramham, P. F. Worley, M. J. Moore, and J. F. Guzowski, "The immediate early gene arc/arg3. 1: regulation, mechanisms, and function," *Journal of Neuroscience*, vol. 28, no. 46, p. 11760, 2008.

[66] T. Miyashita, S. Kubik, G. Lewandowski, and J. F. Guzowski, "Networks of neurons, networks of genes: an integrated view of memory consolidation," *Neurobiology of learning and memory*, vol. 89, no. 3, pp. 269–284, 2008.

[67] M. Knobloch and I. M. Mansuy, "Dendritic Spine Loss and Synaptic Alterations in Alzheimer's Disease," *Molecular Neurobiology*, vol. 37, no. 1, pp. 73-82, 2008.

[68] K. Hayashi and T. Shirao, "Change in the shape of dendritic spines caused by overexpression of drebrin in cultured cortical neurons," *Journal of Neuroscience*, vol. 19, no. 10, p. 3918, 1999.

[69] Peitsch et al., "Drebrin particles: components in the ensemble of proteins regulating actin dynamics of lamellipodia and filopodia.," *European Journal of Biology*, vol. 9, no. 80, pp. 567-79, 2001.

[70] K. Hayashi et al., "Modulatory role of drebrin on the cytoskeleton within dendritic spines in the rat cerebral cortex," *Journal of Neuroscience*, vol. 16, no. 22, p. 7161, 1996.

[71] H. Takahashi, Y. Sekino, S. Tanaka, T. Mizui, S. Kishi, and T. Shirao, "Drebrin-dependent actin clustering in dendritic filopodia governs synaptic targeting of postsynaptic density-95 and dendritic spine morphogenesis," *Journal of Neuroscience*, vol. 23, no. 16, p. 6586, 2003.

[72] K. S. Shim and G. Lubec, "Drebrin, a dendritic spine protein, is manifold decreased in brains of patients with Alzheimer's disease and Down syndrome," *Neuroscience letters*, vol. 324, no. 3, pp. 209–212, 2002.

[73] N. Kojima and T. Shirao, "Synaptic dysfunction and disruption of postsynaptic drebrin-actin complex: a study of neurological disorders accompanied by cognitive deficits," *Neuroscience research*, vol. 58, no. 1, pp. 1–5, 2007.

[74] F. Calon et al., "Docosahexaenoic acid protects from dendritic pathology in an Alzheimer's disease mouse model," *Neuron*, vol. 43, no. 5, pp. 633–645, 2004.

[75] B. Li, Y. Otsu, T. H. Murphy, and L. A. Raymond, "Developmental decrease in NMDA receptor desensitization associated with shift to synapse and interaction with postsynaptic density-95," *Journal of Neuroscience*, vol. 23, no. 35, p. 11244, 2003.

[76] Y. Lin, V. A. Skeberdis, A. Francesconi, M. V. Bennett, and R. S. Zukin, “Postsynaptic density protein-95 regulates NMDA channel gating and surface expression,” *Journal of Neuroscience*, vol. 24, no. 45, p. 10138, 2004.

[77] A. E. El-Husseini, E. Schnell, D. M. Chetkovich, R. A. Nicoll, and D. S. Bredt, “PSD-95 involvement in maturation of excitatory synapses,” *Science*, vol. 290, no. 5495, p. 1364, 2000.

[78] M. L. Kramer and W. J. Schulz-Schaeffer, “Presynaptic alpha-synuclein aggregates, not Lewy bodies, cause neurodegeneration in dementia with Lewy bodies,” *The Journal of Neuroscience: The Official Journal of the Society for Neuroscience*, vol. 27, no. 6, pp. 1405-1410, Feb. 2007.

[79] S. Zaja-Milatovic et al., “Dendritic degeneration in neostriatal medium spiny neurons in Parkinson disease,” *Neurology*, vol. 64, no. 3, p. 545, 2005.

[80] F. Engert and T. Bonhoeffer, “Dendritic spine changes associated with hippocampal long-term synaptic plasticity,” *J. Physiol*, vol. 260, pp. C917–925, 1991.

[81] T. A. Lanz, D. B. Carter, and K. M. Merchant, “Dendritic spine loss in the hippocampus of young PDAPP and Tg2576 mice and its prevention by the ApoE2 genotype,” *Neurobiology of disease*, vol. 13, no. 3, pp. 246–253, 2003.

[82] T. L. Spires-Jones et al., “Impaired Spine Stability Underlies Plaque-Related Spine Loss in an Alzheimer's Disease Mouse Model,” *American Journal Of Pathology*, vol. 171, no. 4, pp. 1304-1311, 2007.

[83] Rosellini, F., Tirard, M., Lu, J., Hutzler, P., Lamberti, p:, and Livrea, P., “Soluble beta-Amyloid1-40 Induces NMDA-Dependent Degradation of Postsynaptic Density-95 at Glutamatergic Synapses,” *Journal of Neuroscience*, no. 25, pp. 11061-11070, 2005.

[84] R. M. Koffie et al., “Oligomeric amyloid beta associates with postsynaptic densities and correlates with excitatory synapse loss near senile plaques,” *Proceedings of the National Academy of Sciences*, vol. 106, no. 10, p. 4012, 2009.

[85] M. Meyer-Luehmann et al., “Rapid appearance and local toxicity of amyloid-β plaques in a mouse model of Alzheimer’s disease,” *Nature*, vol. 451, no. 7179, pp. 720-724, 2008.

[86] A. Iwai et al., “The precursor protein of non-A beta component of Alzheimer's disease amyloid is a presynaptic protein of the central nervous system,” *Neuron*, vol. 14, no. 2, pp. 467–475, 1995.

[87] E. Masliah et al., “beta-Amyloid peptides enhance alpha-synuclein accumulation

and neuronal deficits in a transgenic mouse model linking Alzheimer's disease and Parkinson's disease," *Proceedings of the National Academy of Sciences of the United States of America*, vol. 98, no. 21, p. 12245, 2001.

[88] F. Yang, K. Uéda, P. P. Chen, K. H. Ashe, and G. M. Cole, "Plaque-associated alpha-synuclein (NACP) pathology in aged transgenic mice expressing amyloid precursor protein," *Brain research*, vol. 853, no. 2, pp. 381–383, 2000.

[89] H. Dong, M. V. Martin, S. Chambers, and J. G. Csernansky, "Spatial relationship between synapse loss and beta-amyloid deposition in Tg2576 mice," *The Journal of comparative neurology*, vol. 500, no. 2, pp. 311–321, 2007.

[90] T. L. Spires et al., "Dendritic spine abnormalities in amyloid precursor protein transgenic mice demonstrated by gene transfer and intravital multiphoton microscopy," *Journal of Neuroscience*, vol. 25, no. 31, p. 7278, 2005.

[91] P. Cras, M. A. Smith, P. L. Richey, S. L. Siedlak, P. Mulvihill, and G. Perry, "Extracellular neurofibrillary tangles reflect neuronal loss and provide further evidence of extensive protein cross-linking in Alzheimer disease," *Acta neuropathologica*, vol. 89, no. 4, pp. 291–295, 1995.

[92] T. Gómez-Isla et al., "Neuronal loss correlates with but exceeds neurofibrillary tangles in Alzheimer's disease," *Annals of neurology*, vol. 41, no. 1, pp. 17–24, 1997.

[93] C. Duyckaerts, B. Delatour, and M. Potier, "Classification and basic pathology of Alzheimer disease," *Acta Neuropathologica*, vol. 118, no. 1, pp. 5-36, 2009.

[94] D. Van Dam et al., "Analysis of cholinergic markers, biogenic amines, and amino acids in the CNS of two APP overexpression mouse models," *Neurochemistry international*, vol. 46, no. 5, pp. 409–422, 2005.

[95] O. Wirths and T. A. Bayer, "Neuron Loss in Transgenic Mouse Models of Alzheimer's Disease," 2010.

Table of Figures

„Ich habe mich bemüht, sämtliche Inhaber der Bildrechte ausfindig zu machen und ihre Zustimmung zur Verwendung der Bilder in dieser Arbeit eingeholt. Sollte dennoch eine Urheberrechtsverletzung bekannt werden, ersuche ich um Meldung bei mir.“

Abbreviations

aa	amino acid
Aβ	amyloid beta
ACh	acetylcholine
AD	Alzheimer's Disease
AMPAR	α-amino-3-hydroxy-5-methyl-4-isoxazolepropionic acid receptor
APS	ammonium persulfate
APO E4	apolipoprotein epsilon 4
APP	amyloid precursor protein
AR	antigen retrieval
ARC/Arg3.1	activity-regulated cytoskeleton-associated protein
biot.	biotinylated
BSA	bovine serum albumin
°C	degree celsius
CA1	cornu ammonis 1
CAA	cerebral amyloid angiopathy
cDNA	complementary DNA
CNS	central nervous system
COMT	catechol-O-methyl transferase
CR	congo red
C-terminus	carboxy terminus
CTX	cortex
DAB	3,3´-diaminobenzidine
DAPI	4´,6-diamidino-2-phenylindole
ddH_2O	double distilled water
DLB	dementia with lewy bodies
DNA	deoxyribonucleic acid
DNase	deoxyribonuclease
dNTP	deoxynucleoside triphosphate
Drebrin	developmentally regulated brain protein
dsDNA	double strand deoxyribonucleic acid
ECL	enhanced chemiluminescence
EDTA	ethylene diamine tetraacedic acid
EGF	epidermal growth factor
ELISA	enzyme linked immunosorbent assay
Fig.	figure
FITC	fluoresceinisothiocyanat
FTDP-17	frontotemporal dementia and parkinsonism linked to chromosome 17
g	gravitational acceleration
GFAP	glial fibrillary acidic protein
GFP	green fluorescent protein
Guanidin-HCl	guanidin-hydrochloride
h	hour
HC	hippocampus
HCl	hydrochloride
HRP	horse radish peroxidase
IF	Immunfluorescence
IHC	immunohistochemistry
KCl	potassium chloride
kD	kilo Dalton

KH_2PO_4	monopotassium phosphate
KO	knock out
LTD	Long Term Depression
LTP	Long Term Potentiation
mA	milliAmpere
MAGUK	membrane-associated guanylate kinase
MAP2	microtubuli associated protein 2
mg	milligram
$MgCl_2$	magnesium chloride
min	minutes
ml	millilitre
mRNA	messenger ribonucleic acid
ms	mouse
MW	Molecular Weight
NAC	non amyloid component
Na_2HPO_4	disodium phosphate
NaOH	sodium hydroxide
neg.	negative
ng	nanogram
NMDAR	N-methyl D-aspartate receptor
N-terminus	amino-terminus
OD	Optical Density
ON	over night
PAGE	polyacrylamide gel electrophoresis
PBS	phosphate buffered saline
PBST	phosphate buffered saline tween
PD	Parkinson's Disease
PCR	polymerase chain reaction
PFA	paraformaldehyde
pg	picogram
PS	presenilin
PSD95	postsynaptic density 95
PSP	progressive supranuclear palsy
rb	rabbit
rec.	recombinant
RNA	ribonucleic acid
Rnase	ribonuclease
RT	room temperature
rpm	rounds per minute
sAPPα	secreted amyloid precursor protein α
SD	Standard Deviation
SDS	sodiumdodecylsulphate
SEM	standard error of the mean
TAE	Tris acetic acid EDTA
tg	transgene
V	Volt
WB	Western Blotting
wt	wildtype
ww	wet weight
µg	microgram
µl	microlitre

Danksagung

Hiermit möchte ich allen danken, die mich während meiner Diplomarbeit bei AFFiRiS AG unterstützt haben und zu deren Gelingen beigetragen haben.

Allen voran möchte ich mich bei Markus Mandler für die Bereitstellung und Betreuung des sehr interessanten Themas und die vielen lehrreichen und geduldigen Diskussionen bedanken.

Zudem danke ich Frank Mattner und Walter Schmidt, die mir ermöglichten bei AFFiRiS AG meine Diplomarbeit zu machen.

Außerdem danke ich Univ.-Prof. Dr. Thomas Decker für die Betreuung der Diplomarbeit auf der Universität Wien.

Besonders möchte ich Rainer Winter für die unermüdliche und ausdauernde Unterstützung bei den Bildanalysen und für die Programmierung der benötigten Makros danken.

Für die gute Zusammenarbeit danke ich meinen Kollegen in der Neurodegeneration Gruppe. Für die stets sehr heiteren Stunden in Büro und Labor bedanke ich mich herzlich bei der Studentenriege Thomas, Kristina und Rebecca sowie bei den lieben Kollegen Claudia, Andrea D. und Nok (Danke für die köstliche Verpflegung!). Für die vielen hilfreichen wissenschaftlichen Anregungen und Feedbacks danke ich Gergana Galabova und Benjamin Reutterer.

Mein besonderer Dank gilt meiner Familie für die jahrelange finanzielle und seelische Unterstützung.
Zu guter Letzt danke ich meinem Markus für Alles.

Curriculum Vitae

Name: Anna Gottenöf

Date of Birth: September, 15th 1984

Place of Birth: Munich, Germany

Nationality: German

Email a0508850@unet.univie.ac.at

Special skills: very good knowledge of spoken and written English, good knowledge of spoken and written Italian, modest knowledge of spoken and written French, very good knowledge of MS-Office

Education:

01/2010-12/2010	Diploma Thesis at the Neurodegeneration Department, AFFiRiS AG, Vienna "*Characterisation of neuropathologic alterations following active immunotherapy against Aβ*" ELISA, SDS-PAGE, WB, Immunohistochemistry, Image Analysis, PCR, DNA extraction
11/2009 – 12/2009	Practical at the Neurodegeneration Department, AFFiRiS AG, Vienna "*Inclusion body myositis – Investigation of pathologic hallmarks in Tg2576 mice*" Immunohistochemistry, ELISA, PCR, DNA extraction
07/2009	Practical training in the Group of Univ.-Prof. Dr. Bläsi, Department for Microbiology, Immunology and Genetics, Max F. Perutz Laboratories

	"*Investigation of the function of a/eIF2 in 4 different Archaea strains*" Plasmid restriction and ligation, cloning in *E.coli*, agarose gel electrophoresis
03/2009 – 10/2009	Student job at AFFiRiS AG, Vienna Preparation on tissue sections using the microtome, buffer preparation
07/2008 – 09/2008	Internship at Olympus Life Science Research Europa GmbH; Munich Support with the establishment of PCR-Kits PCR, RT-PCR, qPCR, PAGE
09/2007 - 02/2008	Studentship of the European student exchange program ERASMUS at Roma3, Rome, Italy
since 10/2005	Academic studies of Biology, Genetics/Microbiology, main focus on Immunology at the University of Vienna
10/2004 – 09/2005	Studies of Business Mathematics, LMU, Munich
06/2004	Leaving Examination (Abitur)
09/1995 – 06/2004	Grammar School, Theresiengymnasium, Munich
09/1991 – 08/1995	Elementary School, Klenzestr., Munich